

1 ***Atherfieldastacus rapax* (Harbort, 1905) (Glypheidae, Mecochiridae) from the Lower**  
2 **Cretaceous of the Maestrat Basin (NE Spain)**

3

4 Oscar González-León<sup>\*1</sup>; Àlex Ossó<sup>2</sup>; Telm Bover-Arnal<sup>3</sup>; Josep Anton Moreno-Bedmar<sup>4</sup>;  
5 Gianluca Frijia<sup>5</sup>; Francisco J. Vega<sup>4</sup>

6

7 1: Posgrado en Ciencias de la Tierra, Universidad Nacional Autónoma de México, México  
8 CdMx. 04510, México and Facultad de Estudios Superiores Iztacala, UNAM, Tlalnepantla,  
9 Estado de México, 54070, Mexico; e-mail: oscar.gonzalez@unam.mx

10 2: Josep V. Foix, 12-H, 1er-1a 43007, Tarragona, Catalonia; e-mail: aosso@comt.cat

11 3: Departament de Mineralogia, Petrologia i Geologia Aplicada, Facultat de Ciències de la  
12 Terra, Universitat de Barcelona, Martí i Franquès s/n, 08028, Barcelona, Spain; e-mail:  
13 telm.boverarnal@ub.edu

14 4: Instituto de Geología, Universidad Nacional Autónoma de México, Ciudad Universitaria,  
15 Coyoacán, CdMx. 04510, Mexico; e-mails: josepamb@geologia.unam.mx,  
16 [vegver@unam.mx](mailto:vegver@unam.mx)

17 5: Department of Earth Sciences, Sultan Qaboos University, Al-Khod, 123 Muscat, Oman;  
18 e-mail: [gfrijia@squ.edu.om](mailto:gfrijia@squ.edu.om)

19

20 \*Corresponding author. Tel.: +52 56231265, E-mail address: oscar.gonzalez@unam.mx

21

22

23 **ABSTRACT**

24 Three specimens of the lobster *Meyeria rapax*, which represent the first record of this  
25 species in Spain were collected in the Artoles Formation cropping out in the surroundings

26 of the town of Ares del Maestrat in the Maestrat Basin. Microfacies and paleontological  
27 analyses of the sedimentary succession containing the fossil lobsters allow us to infer a  
28 near-coastal depositional setting. Numerical ages derived from Sr-isotope analyses  
29 combined with previous chronostratigraphic studies of the Artoles Formation suggest an  
30 Early Barremian age for the stratigraphic interval, which is located around the middle part  
31 of the formation, with lobsters studied. The study of the morphological features observed in  
32 the record of the *Meyeria rapax* specimens from Spain supports the ascription of the  
33 species to the new genus *Atherfieldastacus* proposed recently for the Mecochiridae family.

34

35 **Keywords:** Mecochiridae; Lobsters; *Meyeria*; *Atherfieldastacus*; Strontium-isotope  
36 stratigraphy; Lower Cretaceous; Spain.

37

## 38 1. INTRODUCTION

39 Glypheidean lobsters (Decapoda, Glypheidea) belong to a particularly specialized  
40 group of decapod crustaceans, which are highly diversified in the fossil record  
41 (Charbonnier et al., 2015), despite their low preservation potential when compared to other  
42 marine invertebrates (Kidwell and Flessa, 1995). In particular, the Mecochiridae family  
43 (Van Straelen, 1925) has been the subject of many studies in recent times (Neto de  
44 Carvalho et al., 2003; Amati et al., 2004; Neto de Carvalho et al., 2007; Feldmann et al.,  
45 2007; Vega et al., 2008; Garassino et al., 2009; López-Horgue, 2009; De Grave et al., 2009;  
46 Schweitzer et al., 2010; Astrop, 2011; González-León et al., 2014, 2015; Charbonnier et al.,  
47 2015; Breton et al., 2015; González-León et al., 2016; Neto de Carvalho, 2016 and Robin et  
48 al., 2016). Mecochiridae is considered to have 48 species within 7 genera (Schweitzer et al.,

49 2010). One of these genera, *Meyeria* M'Coy, 1849, until recently included 10 species:  
50 *Meyeria ornata* (Phillips, 1829); *Meyeria magna* M'Coy, 1849; *Meyeria harveyi*  
51 (Woodward, 1900); *Meyeria rapax* (Harbort, 1905); *Meyeria schwarzi* (Kitchin, 1908);  
52 *Meyeria bolivari* (Van Straelen, 1927); *Meyeria gracilis* (Glaessner, 1932); *Meyeria*  
53 *mexicana* (Rathbun, 1935); *Meyeria houdardi* (Van Straelen, 1936) and *Meyeria crofti*  
54 (Ball, 1960). Nevertheless, in a recent work, Robin et al. (2016) proposed to include a new  
55 genus within the family Mecochiridae, (*Atherfieldastacus* Simpson in Robin et al., 2016)  
56 based on some particular characteristics which are absent or modified in *Meyeria* and  
57 *Mecochirus*. Due to these morphological differences, these authors proposed that some  
58 species of the former *Meyeria* must be attributed to the new genus *Atherfieldastacus*:  
59 *Atherfieldastacus magnus* (M'Coy, 1849); *Atherfieldastacus mexicanus* (Rathbun, 1935);  
60 *Atherfieldastacus rapax* (Harbort, 1905) and *Atherfieldastacus schwartzi* (Kitchin, 1908).

61 The current work is the first report of *Meyeria rapax* in Spain and analyzes the  
62 inclusion of the species *M. rapax* under the genus *Atherfieldastacus*. This species has a  
63 wide distribution, despite not occurring abundantly in the geological record. *M. rapax* has  
64 been known from the early Valanginian of Germany (Harbort, 1905; Glaessner, 1932);  
65 Hauterivian, Speeton Clay and Tealby Clay, England (Woods, 1928); and the late  
66 Valanginian-early Hauterivian from the Neuquén Basin in Argentina (Aguirre-Urreta,  
67 1985, 1989 and 2003). In addition, the occurrence of this species has been reported in the  
68 lower Barremian of Lusitanian Basin, Portugal (Neto de Carvalho et al., 2003, 2007 and  
69 Neto de Carvalho, 2016). The herein studied specimens of *A. rapax* were collected in the  
70 Lower Cretaceous of the Artoles Formation, Maestrat Basin, in a sedimentary succession  
71 outcropping in the municipal district of Ares del Maestrat (Comarca of l'Alt Maestrat),  
72 northeast Spain (Fig. 1). In order to establish a proper stratigraphic and chronostratigraphic

73 framework of the first Spanish record of *A. rapax* we describe the stratigraphic section that  
74 contains this lobster record and we analyse the microfacies, and the micro and  
75 macropalaeontological record. Any macro or micro-fossils identified in the studied section  
76 do not have a precise biostratigraphic value. For this reason, we collected oyster shells in  
77 order to obtain an age-calibration by means of strontium-isotope stratigraphy.

78

## 79 **2. GEOLOGICAL SETTING**

80 The Maestrat Basin developed in the eastern margin of the Iberian plate due to  
81 tectonic extension of terminal Oxfordian (Late Jurassic)-early Late Albian (Early  
82 Cretaceous) age (Salas and Casas, 1993; Salas et al., 2001, 2010). This rifting episode  
83 resulted from the opening and spreading of the Neotethys towards the west, and the  
84 opening of the Central Atlantic Ocean and the Bay of Biscay (Salas and Casas, 1993; Salas  
85 et al., 2001, 2010). Along this rifting event, the Maestrat Basin was compartmentalized into  
86 seven sub-basins: Aliaga, El Perelló, Morella, Oliete, Galve, Penyagolosa and La Salzedella  
87 (Salas and Guimerà, 1996; Fig. 1B). Later on, and owing to the Alpine contraction, the  
88 Maestrat Basin was inverted and gave rise to the eastern part of the Iberian Chain during  
89 the Late Eocene-Early Miocene (Salas et al., 2001; Nebot and Guimerà, 2016; Fig. 1A).

90 The fossil lobster specimens studied here were sampled in La Salzedella sub-basin  
91 (Fig. 1B), in a cut of the road CV-15, which goes from Vilafranca to Ares del Maestrat  
92 (Fig. 1C). The stratigraphic succession examined belongs to the Artoles Formation defined  
93 by Salas (1987). This lithostratigraphic unit mainly corresponds to marine shallow-water  
94 marls, sandy limestones and limestones rich in oysters (Salas, 1987; Bover-Arnal et al.,  
95 2016). The Artoles Formation has been classically attributed to the Barremian Stage (Salas,  
96 1987; Salas et al., 2001; Bover-Arnal et al., 2016), although a latest Hauterivian age for its

97 lowermost part in the depocenter of the basin, such as La Salzedella sub-basin (Fig. 1B), is  
98 not discarded (Esnaola and Canérot, 1972; Canérot and Pignatelli García, 1977; Salas et al.,  
99 2001). See Salas et al. (2001) and Bover-Arnal et al. (2016) for detailed chronostratigraphic  
100 charts of the Early Cretaceous of the Maestrat Basin.

101

### 102 **3. SEDIMENTOLOGY AND PALEONTOLOGICAL CONTENT OF THE** 103 **SUCCESSION**

104 The sedimentary record studied corresponds to a 20.35 m thick alternation of marls,  
105 marly limestones and limestones (Figs. 2 and 3A). The first 1.8 m of this succession are  
106 constituted by two beds of decimeter – to-meter thickness, with a grainstone texture that is  
107 capped by a hardground (Fig. 2). These grainstones are poorly sorted and rich in peloids,  
108 ooids (Fig. 3B), grapestones, gastropods, fragments of oysters, other bivalves, fragments of  
109 echinoids and bryozoans, miliolids, *Choffatella decipiens* Schlumberger, 1905 (Fig. 3C),  
110 *Pseudocyclamina*, textularids, encrusting foraminifera, other undetermined benthic  
111 foraminifera, and in sections serpulids and dasycladaceans (Fig. 3D). Saddle dolomite and  
112 silt-sized quartz grains occur. Above the hardground, there is an 85 cm-thick bed with  
113 oysters, other bivalves, gastropods and fragments of echinoids. The texture is mainly  
114 floatstone, but in the uppermost part it corresponds to a cm-thick framestone (Fig. 3E)  
115 made up of oysters, serpulids (Fig. 3F) and encrusting foraminifera.

116 From meter 2.65 to meter 11.1 (Fig. 2), the marly limestones and limestones exhibit  
117 wackestone, floatstone and rudstone textures with oysters and other bivalves as dominant  
118 skeletal components. The marl intervals contain abundant oysters and other undetermined  
119 bivalves. *Gastrochaenolites* borings, at times preserving the shell of the lithophagid bivalve  
120 (Fig. 3G), are frequent in these bioclasts. Other common components present in this

121 stratigraphic interval are peloids, gastropods, fragments of echinoids, serpulids,  
122 dasycladaceans and bryozoans, *Trocholina* and other benthic foraminifera. At meter 9.35,  
123 millimeter-sized rock fragments occur (Fig. 4A). *Thalassinoides*, as well as other burrows,  
124 are widespread throughout this lower part of the succession investigated.

125         At meter 11.1, a 40 cm-thick bed made up of a floatstone to rudstone texture  
126 dominated by fragments of oysters, other bivalves and gastropods occurs. This bed also  
127 includes specimens of *Atherfieldastacus rapax* (Fig. 2), ooids, coated grains, peloids,  
128 fragments of echinoids, crushing teeth of pycnodont, as well as mud nodules. Following a  
129 1.5 m-thick covered outcrop interval (Fig. 2), the succession corresponds to an alternation  
130 between marls, marly limestones and limestones with floatstone to rudstone textures  
131 (meters 13-16.45; Fig. 2). The components giving rise to these latter textures are fragments  
132 and wholly preserved shells of oysters, other bivalves, gastropods and serpulids. Fragments  
133 of mollusks are commonly bioeroded. Coated grains, ooids, peloids and fragments of  
134 echinoids also occur. Large *Thalassinoides* (Fig. 4B) and other burrows are widespread in  
135 this interval.

136         A 30 cm-thick floatstone to rudstone limestone bed capped by a hardground with  
137 encrusting oysters is found at meter 16.45 (Fig. 2). The bed is composed of fragments of  
138 oysters, other bivalves, gastropods, echinoids, corals (Fig. 4C), serpulids and rocks, as well  
139 as benthic foraminifera and coated grains. Above, marls, and marly limestones and  
140 limestones with wackestone, packstone and floatstone textures, alternate. These deposits,  
141 which occur between meter 16.45 and meter 19.85 (Fig. 2), are very rich in oysters and  
142 show frequent bioturbation by *Thalassinoides* and other burrows. Other common  
143 components in the marly limestones and limestones of the upper part of the strata  
144 investigated include other bivalves, which are at times bioeroded, gastropod shells,

145 serpulids, encrusting foraminifera and fragments of dasycladaceans and echinoids. From  
146 meter 16.95 to meter 17.3, specimens of *Atherfieldastacus rapax* are also found (Fig. 2). At  
147 meter 17.25, a razor shell was identified (Fig. 4D).

148 The top of the stratigraphic succession investigated is marked by a 50 cm-thick  
149 tabular limestone bed with a wackestone to packstone texture dominated by fragments of  
150 oysters, other bivalves, gastropods (Fig. 4E) and echinoids. Occasionally, the mollusk  
151 shells are bioeroded. Peloids, coated grains, benthic foraminifera, and fragments of  
152 bryozoans, serpulids, dasycladaceans and crinoids (Fig. 4F) also occur. The base of this  
153 uppermost bed is characterized by the presence of large *Thalassinoides* burrows.

154

#### 155 **4. SR-ISOTOPE ANALYSIS AND AGE OF THE *ATHERFIELDASTACUS RAPAX*** 156 **STUDIED**

157 The age of the specimens studied has been constrained by means of Sr-isotope  
158 stratigraphy, see Steuber (1999, 2001), McArthur and Howard (2004), Steuber et al. (2005),  
159 Frijia and Parente (2008), Bodin et al. (2009), Boix et al. (2011), Frijia et al. (2015) for  
160 detailed reviews on this chemostratigraphic method.

161 The two shells of oysters (V4A and V4B) used for Sr-isotope stratigraphy come  
162 from a bed very rich in these bivalves located at 2.65 meters in the sedimentary succession  
163 logged (Fig. 2). This bed is approximately 8.45 and 14.35 meters below the two beds with  
164 the identified *A. rapax* (Fig. 2).

165 The preservation of the analysed fossils was evaluated using an accurate diagenetic  
166 screening following the procedure described in detail in previous works (Steuber et al.,  
167 2005; Boix et al., 2011; Frijia et al., 2015). Trace element analysis (high Sr content versus  
168 low Mn and Fe concentrations; Table 1) and petrographic observations show no evidence

169 of significant diagenetic alteration of the oyster shells, suggesting that they preserve their  
170 pristine chemical composition. Furthermore, internal consistency of the Sr-isotope ratios of  
171 the two shell fragments reinforces the hypothesis that they preserve the original Sr-isotope  
172 signature of seawater (Table 1).

173 The  $^{87}\text{Sr}/^{86}\text{Sr}$  value of  $0.707472 \pm 0.000011$  obtained from the analysed samples  
174 when compared with the  $^{87}\text{Sr}/^{86}\text{Sr}$  reference curve for Cretaceous seawater (McArthur et al.  
175 2001; age derived using the look-up table version 4: 08/04) translates into two possible  
176 ages: one of 126.46 Ma (-0.6/+0.74; Table 1) and a second of 130.43 Ma (-1.89/+1.4; Table  
177 1). The first age corresponds to the Late Barremian whereas the second to the latest  
178 Hauterivian-Early Barremian time interval (Gradstein et al., 2004).

179 The existing chronostratigraphic frameworks for the Lower Cretaceous of the  
180 Maestrat Basin mainly attribute the Artoles Formation to the Barremian (Salas, 1987; Salas  
181 et al., 2001; Bover-Arnal et al., 2016). In addition, in the depocenter of the basin (La  
182 Salzedella sub-basin), the lowermost part of the Artoles Formation could be of latest  
183 Hauterivian age (Esnaola and Canérot, 1972; Canérot and Pignatelli García, 1977; Salas et  
184 al., 2001). Therefore, both preferred ages are possible considering the associated errors  
185 (Table 1). However, according to the numerical age dataset presented by Bover-Arnal et al.  
186 (2016), the preferred age of 126.46 Ma (-0.6/+0.74) mainly falls into the numerical age  
187 domain of the Late Barremian Morella, Cervera del Maestrat and Xert formations, which  
188 stratigraphically overlay the Artoles Formation. On the other hand, the associated  
189 maximum age of 127.27 Ma (Table 1) would fall into the numerical age domain of the  
190 uppermost part of the Artoles Formation (Bover-Arnal et al., 2016). However, given that  
191 the succession studied corresponds to a stratigraphic interval located around the middle part  
192 of the formation, this possibility seems unlikely.

193 Accordingly, we favour the preferred age of 130.43 Ma (-1.89/+1.4; Table 1). Nevertheless,  
194 given that the rocks investigated are located in the middle Artoles Formation, a latest  
195 Hauterivian age for this stratigraphic interval is improbable according to previous studies  
196 on the age assignation of the Artoles Formation (Salas, 1987; Salas et al., 2001; Bover-  
197 Arnal et al., 2016). Therefore, an Early Barremian age (130-128.54 Ma) is assigned to the  
198 oysters analyzed for Sr-isotope stratigraphy and the beds with *A. rapax* examined in this  
199 study.

200

201 **Acronym:** MGB: Museu de Geologia – Museu de Ciències Naturals de Barcelona MGB-  
202 MCNB (Barcelona, Catalonia).

203

## 204 **5. SYSTEMATIC PALEONTOLOGY**

205

206 Order Decapoda Latreille, 1802

207 Suborder Pleocyemata Burkenroad, 1963

208 Infraorder Glypheidea von Zittel, 1885

209 Superfamily Glypheoidea von Zittel, 1885

210 Family Mecochiridae Van Straelen, 1925

211 Genus: *Atherfieldastacus* Simpson in Robin et al., 2016

212

213 **Type species.** — *Meyeria magna* M'Coy, 1849.

214

215 **Included species.** — *Atherfieldastacus magnus* (M'Coy, 1849) — *Atherfieldastacus*  
216 *mexicanus* (Rathbun, 1935) — *Atherfieldastacus rapax* (Harbort, 1905) —  
217 *Atherfieldastacus schwartzi* (Kitchin, 1908).

218

## 219 **5.1 DIAGNOSIS OF THE NEW GENUS *ATHERFIELDASTACUS* SIMPSON IN**

220 **ROBIN ET AL. (2016)** — Subcylindrical carapace, laterally compressed, about two-thirds  
221 the length and twice the height of pleon; carapace with bevelled, sublanceolate cross  
222 section; short pointed rostrum, spineless; branchial region with three lateral branchial ridges  
223 broadening the carapace: dorsal branchial ridge (r2) between postcervical and  
224 branchiocardiac grooves; medial branchial ridge (r3), curved and parallel to posterior  
225 margin; ventral branchial ridge (r1), extending hepatic carina; antennal pterygostomial  
226 region with strongly concave ventral margin; cervical groove strongly oblique, ventrally  
227 joined to antennal groove, delimiting narrow cephalic region; cephalic region with  
228 longitudinal carinae; short gastro-orbital groove originating as a slight inflexion of the  
229 cervical groove at level of gastro-orbital carina; postcervical and branchiocardiac grooves  
230 parallel, directed toward the posterior margin; postcervical groove joined ventrally to  
231 branchiocardiac groove, forming one elongated lobe crossed by dorsal branchial ridge (r2);  
232 straight cardiac groove, forward-inclined and joined posteriorly to postcervical groove;  
233 cardiac groove joined to dorsal margin; hepatic region with tuberculated longitudinal  
234 hepatic carina above hepatic groove, and prolonged by ventral branchial ridge (r1) in  
235 branchial region; hepatic groove shallow and curved toward posterior; short inferior groove  
236 joined to hepatic groove, and connected to ventral margin; subchelate P1–P2; achelate P3–  
237 P5; very elongated P1; uropodal exopod with diaeresis; uropodal endopod with fibrous and  
238 flexible distal portion.

239

240 *Atherfieldastacus rapax* (Harbort, 1905)

241 Figures 5, 6, 7, 8 and 9A

242

243 pars 1863 *Astacodus falcifer* Phillips Bell, p. 30, pl. 9, fig. 3 only.

244 \*1905 *Meyeria rapax* Harbort, 1905, p. 11, pl. 1, fig. 12; pl. 2, figs. 1a-c, 2a-b, 3-4.

245 1928 *Meyeria rapax* Harbort, 1905; Woods, p. 70, pl. 18, figs. 5?, 6, 7?, 8.

246 1932 *Meyeria rapax* Harbort, 1905; Glaessner, p. 58.

247 1976 *Mecochirus rapax* Harbort, 1905; Kemper, pl. 11, fig. 1.

248 1985 *Meyeria rapax* Harbort, 1905; Aguirre-Urreta, pl. 1, figs. D-G.

249 1989 *Meyerella rapax* Harbort, 1905; Aguirre-Urreta, pl. 59, figs. 5-8; text-fig. 18;

250 text-fig. 19.

251 2003 *Meyerella rapax* Harbort, 1905; Aguirre-Urreta, fig.1.

252 2007 *Mecochirus rapax* Harbort, 1905; Neto de Carvalho et al., fig. 2e-g; fig. 3a-b.

253 2016 *Meyeria rapax* Harbort, 1905; Neto de Carvalho, fig. 2e-g; fig. 3b-c; fig. 6.

254

## 255 **5.2 MATERIAL**

256 The three specimens described here as *Atherfieldastacus rapax* consist of a nearly  
257 complete carapace preserving only the right side, and morphological features and regions  
258 that are well defined. A second nearly complete specimen from the same outcrop allows us  
259 to observe details from the carapace, pleon and telson. A third specimen does not present  
260 completely the cephalothorax, only part of the branchial region can be observed. The  
261 abdomen is incomplete and only five abdominal segments are preserved, however, the  
262 telson is relatively well preserved. The specimens are housed in the collection of the

263 Museu de Geologia – Museu de Ciències Naturals de Barcelona (MGB-MCNB)  
264 (Barcelona, Catalonia) with the collection numbers MGB 76814, MGB 76815 and MGB  
265 78616 respectively.

266

267 ***Carapace anatomical abbreviations.*** a = branchiocardiac groove, ac = antennal carina,  
268 b = antennal groove, b<sub>1</sub> = hepatic groove = c = post-cervical groove, cd = cardiac groove,  
269 e<sub>1</sub>e = cervical groove, gc = gastro-orbital carina, hr = hepatic ridge, i = inferior groove, oc =  
270 orbital carina. Regions of the carapace (colors): blue = branchial region, green = hepatic  
271 region, yellow = pterygostomial region, orange = antennal region, red = gastric region,  
272 purple = cardiac region (Fig. 5).

273

274 **Locality.** Ares del Maestrat, Artoles Formation, Maestrat Basin, Northeast Spain.

275

### 276 **5.3 DESCRIPTION OF THE SPECIMENS**

277 Regarding the anatomical features and regions of the carapace we follow the  
278 terminology published in Charbonnier et al. (2013) for the glypheideans. For the branchial  
279 carinae terminology we follow González-León et al. (2014).

280

281 ***Carapace.*** Laterally compressed and subcylindrical; cephalic region with three  
282 longitudinal spiny carinae; orbital, gastro-orbital and antennal carina parallel; very short  
283 distance between orbital and gastro-orbital carinae, antennal carina separated four times the  
284 distance from the others; cephalic carinae raised, antennal carina and gastro-orbital carina  
285 more raised than the orbital carinae. Hepatic region: granules above of a hepatic groove  
286 forming a hepatic ridge; between branchiocardiac groove and post-cervical groove there are

287 granules towards the hepatic region forming the branchial ridge (r2) extending towards  
288 hepatic ridge; ventral branchial ridge (r1) not developed; medial branchial ridge (r3) curved  
289 and parallel to posterior margin of carapace. Cervical groove deep, in an average height of  
290 carapace, inclined 44° toward lower anterior margin, cervical groove ventrally connected  
291 to antennal groove; branchiocardiac groove shallow, inclined 18° from upper part of  
292 posterior margin to midheight of carapace; post-cervical groove slightly deep and parallel  
293 to branchiocardiac groove; hepatic groove slightly deep, convex ventrally at intersection  
294 with antennal groove; shallow and undeveloped inferior groove, connected to hepatic  
295 groove. Cuticle of the anterior cardiac region with small tubercles; the entire cuticle of the  
296 branchial region is covered by tubercles of uniform size, coming together toward the  
297 pterygostomial region and the ventral part of the branchial region.

298

299 *Pleon.* Five segments of the abdomen are preserved; abdominal segments with the  
300 smallest tubercles are found in the dorsal region, more evident in the pleural region; first  
301 abdominal segment not well preserved; second abdominal segment with anterior and lower  
302 margin rounded, posterior margin straight; pleura three to five times smaller in size and  
303 triangular; telson with tubercles at the basis, uropodal of endopodite and exopodite  
304 towards the posterior region; uropodal of exopodite with diaeresis.

305

306 *Thoracic appendages.* Pereiopods are partially preserved and exhibit the first slender  
307 and long pereiopods; merus, carpus and propodus evident with two lines of tubercles in the  
308 ventral margin.

309

310 **6. DISCUSSION**

311 We support the inclusion of the *Meyeria rapax* species in the genus  
312 *Atherfieldastacus* on the basis of their morphological features which distinguish them from  
313 the *Meyeria* genus (see Robin et al., 2016 for more detailed explanations about the  
314 morphological differences).

315 The three specimens analyzed here from the Ares del Maestrat in the Maestrat Basin  
316 (Figs. 6, 7 and 9) have many similarities with those published first by Harbort, 1905, and  
317 those published later by Woods, 1928, Aguirre-Urreta, 1989, and recently by Neto de  
318 Carvalho et al., 2003 and Neto de Carvalho, 2016.

319 In figures 6A, C and 7, the specimens of *Atherfieldastacus rapax* present the  
320 development of the dorsal branchial ridge (r2), the medial branchial ridge (r3) and the  
321 development of the hepatic ridge (hr). Nevertheless *A. rapax* does not present the ventral  
322 branchial ridge like other species such as *Atherfieldastacus magnus* and *Atherfieldastacus*  
323 *mexicanus* in which this ridge is connected to the hepatic ridge. The features observed in  
324 the herein studied Spanish specimens are the same as the specimens illustrated by Harbort,  
325 1905 pl. 1, fig. 12; Woods, 1928, pl. 18, fig. 8; Aguirre-Urreta, 1989 pl. 59, figs. 5, 7 and 8;  
326 Neto de Carvalho et al., 2003 fig. 2b and Neto de Carvalho, 2016 fig. 3c.

327 In the figure 6A, B the arrangement and number of spines that form the gastro-  
328 orbital carinae on both sides of the specimen can be observed, having twelve spines that  
329 increase in size towards the anterior part of the rostrum. The orbital carinae consists of  
330 small granules forming a parallel line above the gastro-orbital carinae. *Atherfieldastacus*  
331 *rapax* presents a particular arrangement of the rostral carinae; there is a very short distance  
332 between orbital and gastro-orbital carinae and the antennal carina is separated from the  
333 gastro-orbital carine with almost four times the distance than between the orbital and  
334 gastro-orbital carinae (Fig. 6A, C and D). This can also be observed in the specimens

335 figured by Harbort, 1905 pl. 2 figs. 1a and 4; Woods, 1928 pl. 18, fig. 5-6; Aguirre-Urreta,  
336 1989 pl. 59, fig. 8 and Neto de Carvalho, 2016 fig. 3c. These features are easily  
337 distinguishable compared with the other species of the genus (e.g. *Atherfieldastacus*  
338 *magnus* and the only known specimen of the *A. mexicanus* species) in which the distance  
339 between the three rostral carinae has a similar separation (Fig. 8).

340         The length of the pleon in the specimen MGB 76815 from Artoles Formation is 1.5  
341 times longer than that of the cefhalothorax (Fig. 7). For the specimen MGB 78616 the total  
342 length of the abdomen cannot be observed, but some details of the ornamentation can be  
343 observed in the abdominal pleuras, as well as the uropodal endopodite and exopodite of  
344 telson (Fig. 9A-C).

345         With the objective of confirm the taxonomic features of Spanish specimens, we  
346 compared the specimens studied in this work with specimens of the early Valanginian of  
347 Sachsenhagen locality in Germany located in a private collection (Appendix 1A-C).  
348 Specimens A and B show the short distance between orbital and gastro-orbital carinae.  
349 Distance between gastro-orbital and antennal carinae consist of a greater separation. It is  
350 also clearly observed that the specimens A-C present the dorsal branchial rigde (r2), the  
351 medial branchial ridge (r3) and the hepatic rigde (hr), and like the Spanish specimens they  
352 do not present the ventral branchial ridge.

353         Regarding the species *A. schwartzi*, there is also a very short distance between the  
354 orbital and gastro-orbital carinae and almost four times that distance between the antennal  
355 carinae and the gastro-orbital carinae. This feature is most similar to the *Atherfieldastacus*  
356 *rapax*, according to the drawing published by Kitchin, 1908 (pl. VIII, fig 22). Aguirre-  
357 Urreta previously recognized in 1989 the closeness between *A. rapax* and *A. schwartzi*,  
358 asserting similarities in the ornamentation, patterns of the grooves and age. But in *A.*

359 *schwartzi* the size is smaller and presents a major compression of the cephalothorax that  
360 distinguishes it from *A. rapax*. This closeness could be explained considering different  
361 ontogenetic stages, in which *A. schwartzi* could represent a juvenile stage of *A. rapax*.

362 The features described above are not observed in specimens included within the  
363 genus *Meyeria* according to Robin et al. (2016); therefore, it is feasible to include the  
364 species aforescribed as *Meyeria rapax* within the new genus *Atherfieldastacus* and use  
365 the new combination *Atherfieldastacus rapax* proposed recently by these authors.

366

## 367 **7. ENVIRONMENTAL INTERPRETATION**

368 The alternating marls, marly limestones and limestones including abundant oysters  
369 described previously indicate a near-coastal depositional setting. The presence of ooids, or  
370 other biotic elements such as dasycladaceans or scleractinians, supports a tropical shallow-  
371 marine environment. The packstone, rudstone and grainstone beds mark periods of higher  
372 energy than the marl lithology, and the wackestone and floatstone textures. The occurrence  
373 of large *Thalassinoides* indicates the possible dwelling of this decapod. This has been  
374 suggested based on the evidence of the relationship of *A. rapax* and *Thalassinoides*  
375 *suevicus* recognized in different beds of the Lower Barremian of the Boca do Chapin and  
376 Rivera de Ilhas formations in the Lusitanian Basin, Portugal (Neto de Carvalho et al., 2003  
377 and 2007).

378 The record of this decapod inside of the *Thalassinodes suevicus* burrows in these  
379 formations has been interpreted as massive mortality events (Neto de Carvalho et al., 2007  
380 and Neto de Carvalho, 2016). Neto de Carvalho (2016) also found some specimens of  
381 *Meyeria rapax* without any apparent relation to the burrows, but these specimens were  
382 contemporaries with those preserved in their burrow systems. We did not find the record of

383 the *Atherfieldastacus rapax* inside the burrows recognized as *Thalassinoides* in the Artoles  
384 Formation, but it is highly probable that these fossil traces are related to the infaunal  
385 activity of this lobster.

386

## 387 **8. CONCLUSIONS**

388 Three specimens of the fossil lobster *Meyeria rapax* are described here and ascribed to the  
389 recently proposed genus *Atherfieldastacus*. The fossil material comes from the Artoles  
390 Formation, Ares del Maestrat in the Maestrat Basin (NE Spain). This species is reported for  
391 the first time in Spain. The sedimentology, micro and macropaleontological analyses of the  
392 sedimentary succession containing *Atherfieldastacus rapax* indicate a shallow marine  
393 environment. The Sr-isotope results derived from the analysis of oyster shells in  
394 combination with previous chronostratigraphic data of the Artoles Formation indicate an  
395 Early Barremian age for the strata with the record of the fossil lobster *Atherfieldastacus*  
396 *rapax*. To confirm the taxonomic allocation of the Spanish specimens, we compared the  
397 Spanish specimens with those specimens of the early Valanginian of Sachsenhagen locality  
398 in Germany.

399

## 400 **Acknowledgments**

401 We thank firstly Joaquim Pastó (Masboquera, Catalonia) who discovered the outcrop and  
402 warned us about it. This study was supported by the projects PAPIIT IN107617 (DGAPA,  
403 Universidad Nacional Autónoma de México), the Grup de Recerca Reconegut per la  
404 Generalitat de Catalunya 2014 SGR 251 "Geologia Sedimentària" and CGL2015-69805-P  
405 (MINECO, FEDER, EU). We thank Uwe and Falk Starke for allowing us to use  
406 photographic material of *Meyeria rapax* for comparison as well as Günter Schweigert for

407 their help and support. Oscar González-León thanks the Posgrado en Ciencias de la Tierra,  
408 Instituto de Geología UNAM and CONACyT for a grant for this research.

409

## 410 **9. REFERENCES**

411 Aguirre-Urreta, M.B., 1985. Nuevos glyfeoideos de Argentina y una reseña de otros  
412 crustáceos decápodos cretácicos. Actas IX° Congr. Brasil. Paleont. Fortaleza.

413 Aguirre-Urreta, M.B., 1989. The Cretaceous decapod Crustacea of Argentina and the  
414 Antarctic Peninsula. *Palaeontology*, 32(3), 499–552.

415 Aguirre-Urreta, M.B., 2003. Early Cretaceous decapod Crustacea from the Nequén Basin,  
416 west-central Argentina. *Contributions to Zoology*, 72(2-3), 79–81.

417 Amati, L., Feldmann, R.M., Zonneveld, J., 2004. A New Family of Triassic Lobsters  
418 (Decapoda: Astacidea) from British Columbia and its Phylogenetic Context. *Journal*  
419 *of Paleontology*, 78, 150–168.

420 Astrop, T.I., 2011. Phylogeny and evolution of Mecochiridae (Decapoda: Reptantia:  
421 Glypheoidea): an integrated morphometric and cladistic approach. *Journal of*  
422 *Crustacean Biology*, 31(1), 114–125.

423 Ball, H.W., 1960. Upper cretaceous Decapoda and Serpulida from James Ross Island,  
424 Graham Land. Falkland Islands Dependencies survey. *Scientific Reports*, 24, 1–30.

425 Bell, T., 1863. A monograph of the fossils malacostracous Crustacea of Great Britain. Part  
426 II. Crustacea of the gault and greensand. *Palaeontographical Society Monographs*,  
427 *The Palaeontographical Society, London*, 21 pp.

428 Bodin, S., Fiet, N., Godet, A., Matera, V., Westermann, S., Clément, A., Janssen, N.M.M.,  
429 Stille, P., Föllmi, K.B., 2009. Early Cretaceous (late Berriasian to early Aptian)  
430 palaeoceanographic change along the northwestern Tethyan margin (Vocontian

431 Trough, southeastern France):  $\delta^{13}\text{C}$ ,  $\delta^{18}\text{O}$  and Sr-isotope belemnite and whole-rock  
432 records. *Cretaceous Research*, 30, 1247–1262.

433 Boix, C., Frijia, G., Vicedo, V., Bernaus, J.M., Di Lucia, M., Parente, M., Caus, E., 2011.  
434 Larger foraminifera distribution and strontium isotope stratigraphy of the La Cova  
435 limestones (Coniacian–Santonian, "Serra del Montsec", Pyrenees, NE Spain).  
436 *Cretaceous Research*, 32, 806–822.

437 Bover-Arnal, T., Salas, R., Guimerà, J., Moreno-Bedmar, J.A., 2014. Deep incision on an  
438 Aptian carbonate succession indicates major sea-level fall in the Cretaceous.  
439 *Sedimentology*, 61, 1558–1593.

440 Bover-Arnal, T., Moreno-Bedmar, J.A., Frijia, G., Pascual-Cebrian, R., Salas, R., 2016.  
441 Chronostratigraphy of the Barremian–Early Albian of the Maestrat Basin (E Iberian  
442 Peninsula): integrating strontium-isotope stratigraphy and ammonoid  
443 biostratigraphy. *Newsletters on Stratigraphy*, 49, 41–68.

444 Breton, G., Néraudeau, D., Dépré, E., 2015. Mecochiridae (Crustacea, Decapoda,  
445 Glypheidea) de l'Albienet du Cénomanién de France. *Annales de Paléontologie*,  
446 101, 55–54.

447 Burkenroad, M.D., 1963. The evolution of the Eucarida (Crustacea, Eumalacostraca), in  
448 relation to the fossil record. *Tulane Studies in Geology*, 2, 3–17.

449 Canérot, J., Pignatelli García, R., 1977. Mosqueruela, hoja nº 569. Mapa Geológico de  
450 España 1:50.000. 2ª Serie. 1ª Edición, Servicio de Publicaciones, Ministerio de  
451 Industria y Energía, Madrid.

452 Charbonnier, S., Audo, D., Barriel, V., Garassino, A., Schweigert, G., Simpson, M., 2015.  
453 Phylogeny of fossil and extant glypheid and litogastrid lobsters (Crustacea,  
454 Decapoda) as revealed by morphological characters. *Cladistics*, 31(3), 231–249.

455 Charbonnier, S., Garassino, A., Shcweigert, G., Simpson, M., 2013. A worldwide review of  
456 fossils and extant glypheid and litogastrid lobsters (Crustacea, Decapoda,  
457 *Glypheoidea*). Mémoires du Muséum national d'Histoire naturelle, Paris, 304 p.

458 De Grave, S. *et al.*, 2009. A classification of living and fossil genera of decapod  
459 crustaceans. Raffles Bulletin of Zoology. Supplement No. 21, 1–109.

460 Esnaola, J.M., Canérot, J., Pignatelli García, R., 1972. Albocàsser, hoja nº 570. Mapa  
461 Geológico de España 1:50.000. 2ª Serie. 1ª Edición, Servicio de Publicaciones,  
462 Ministerio de Industria y Energía, Madrid.

463 Feldmann, R.M., Vega, F.J., Martínez-López, L., González-Rodríguez, K.A., González-  
464 León, O., Fernández-Barajas, R.M., 2007. Crustacea from the Muhi Quarry (Albian-  
465 Cenomanian), and a review of Aptian Mecochiridae (Astacidea) from México.  
466 Annals of Carnegie Museum, 76(4), 135–144.

467 Frijia, G., Parente, M., 2008. Strontium isotope stratigraphy in the upper Cenomanian  
468 shallow-water carbonates of the southern Apennines: short-term perturbations of  
469 marine  $87\text{Sr}/86\text{Sr}$  during the oceanic anoxic event 2. Palaeogeography,  
470 Palaeoclimatology, Palaeoecology, 261, 15–29.

471 Frijia, G., Parente, M., Di Lucia, M., Mutti, M., 2015. Carbon and strontium isotope  
472 stratigraphy of the Upper Cretaceous (Cenomanian-Campanian) shallow-water  
473 carbonates of southern Italy: Chronostratigraphic calibration of larger foraminifera  
474 biostratigraphy. Cretaceous Research, 53, 110–139.

475 Garassino, A., Artal, P., Pasini, G., 2009. *Jabaloya aragonensis* n. gen., n. sp. (Crustacea,  
476 Decapoda, Mecochiridae) and *Cedrillosia jurassica* n. gen., n. sp. (Crustacea,  
477 Decapoda, Glypheidae) from the Upper Jurassic of Teruel Province (Aragón,

478 Spain). Atti della Società Italiana di Scienze Naturali e del Museo Civico di Storia  
479 Naturale di Milano, 150(2), 197–206.

480 Glaessner, M.F., 1932. Zwei ungenügend bekannte Mesozoische Dekapodenkrebse,  
481 *Pemphix sueuri* (Desm.) und *Palaeophoberus suevicus* (Quenstedt).  
482 Paläontologische Zeitschrift, 14, 108–121.

483 González-León, O., Moreno-Bedmar, J.A., Vega, F.J., 2014. Morphology and ontogeny of  
484 the fossil lobster *Meyeria magna* M'Coy, 1849 (Astacidae, Mecochiridae) from the  
485 Lower Cretaceous (Lower Aptian) of Mexico, United Kingdom and Spain. Neues  
486 Jahrbuch für Geologie und Paläontologie Abhandlungen, 271(1), 49–68.

487 González-León, O., Jeremiah, J., Schlagintweit, Bover-Arnal, T., Moreno-Bedmar, J.A.,  
488 Mendoza-Rosales, C., Vega, F.J., 2015. Novel contributions and errata of the work  
489 “Morphology and ontogeny of the fossil lobster *Meyeria magna* M'Coy, 1849  
490 (Astacidae, Mecochiridae) from the Lower Cretaceous (Lower Aptian) of Mexico,  
491 United Kingdom and Spain”. Neues Jahrbuch für Geologie und Paläontologie  
492 Abhandlungen, 276(3), 323–334.

493 González-León, O., Patarroyo, P., Moreno-Bedmar, J.A., Nyborg, T., Vega, F.J., 2016. A  
494 new record and cuticular structure of *Meyeria magna* (Decapoda, Mecochiridae)  
495 from the lower Albian (Lower Cretaceous) of Colombia. Cretaceous Research 57,  
496 342–349.

497 Gradstein, F.M., Ogg, J.G., Smith, A.G., 2004. A Geologic Time Scale 2004. Cambridge  
498 University Press, Cambridge, 610 pp.

499 Harbort, E., 1905. Die Fauna der Schaumburg-Lippe'schen Kreidemulde. Abhandlungen  
500 der Preussischen Geologischen Landesanstalt, neue Folge, 14, 10–22.

501 Kemper, E., 1976. Geologischer Führer durch die Grafschaft Bentheim und die  
502 angrenzenden Gebiete mit einem Abriss der emsliindischen Unterkreide (5th edn),  
503 Nordhorn, Bentheim, 206 pp.

504 Kidwell, S.M., Flessa, K.W., 1995. The quality of the fossil record: populations, species,  
505 and communities. *Annual Review of Ecology and Systematics*, 24, 433–464.

506 Kitchin, F.L., 1908. The invertebrate fauna and palaeontological relations of the Uitenhage  
507 series. *Annals of the South African Museum*, 7, 212–268.

508 Latreille, P.A., 1802–1803. *Histoire naturelle, general et particulière des crustacés et des*  
509 *insectes* (vol. 3). Paris: F. Dufart, 468 pp.

510 López-Horgue, M.A., 2009. New occurrences of *Meyeria magna* M’Coy, 1849 (Decapoda,  
511 Mecochiridae) in the early Aptian and early Albian of the Basque Cantabrian Basin  
512 (North Spain). *Geogaceta*, 47, 25–28.

513 McArthur, J.M., Howarth, R.J., Bailey, T.R., 2001. Strontium isotope stratigraphy: lowess  
514 version 3. Best-fit to the marine Sr-isotope curve for 0 to 509 Ma and accompanying  
515 look-up table for deriving numerical age. *Journal of Geology*, 109, 155–170.

516 McArthur, J.M., Howarth, R.J., 2004. Strontium isotope stratigraphy. In: Gradstein, F.,  
517 Ogg, J., Smith, A. (Eds.), *A Geological Time Scale*. Cambridge University Press,  
518 Cambridge, U.K., 96–105.

519 M’Coy, F., 1849. On the classification of some British fossil Crustacea, with notices of new  
520 forms in the University Collection at Cambridge. *The Annals and Magazine of*  
521 *Natural History*, 4(2), 330–335.

522 Nebot, M., Guimerà, J., 2016. Structure of an inverted basin from subsurface and field data:  
523 The Late Jurassic-Early Cretaceous Maestrat Basin (Iberian Chain). *Geologica Acta*,  
524 14, 155–177.

- 525 Neto de Carvalho, C., Viegas, P., Teodoso, B., Cachão, M., 2003. O primeiro registo de  
526 comunidades de *Mecochirus* (Crustacea, Decapoda) sepultadas no interior de  
527 *Thalassinoides* (Barremiano inferior, Formação Boca do Chapim). Actas do VI  
528 Congresso Nacional de Geologia; Ciências da Terra (UNL), nº esp. 5, 32–35.
- 529 Neto de Carvalho, C., Viegas, P., Cachão, M., 2007. *Thalassinoides* and its producer:  
530 Populations of *Mecochirus* Buried within their Burrow System, Boca do Champim  
531 Formation (Lower Cretaceous), Portugal. *Palaios*, 22, 107–112.
- 532 Neto de Carvalho, C., 2016. The massive death of lobsters smothered within their  
533 *Thalassinoides* burrows: the example of the lower Barremian from Lusitanian Basin  
534 (Portugal). *Comunicações Geológicas*, 103, Especial 1, 143–152.
- 535 Phillips, J., 1829. Illustrations of the geology of Yorkshire, Part 1. The Yorkshire coast.  
536 John Murray, London, 184 pp.
- 537 Robin, N., Charbonnier, S., Merle, D., Simpson, M., Petit, G., Fernandez, S., 2016.  
538 Bivalves on mecochirid lobsters from the Aptian of the Isle of Wight: Snapshot on  
539 an Early Cretaceous palaeosymbiosis. *Palaeogeography, Palaeoclimatology,*  
540 *Palaeoecology*, 453, 10–19.
- 541 Rathbun, M.J., 1935. Fossil Crustacea of the Atlantic and Gulf Coastal Plain. Geological  
542 Society of America, Special Paper, 2, 1–160.
- 543 Salas, R., 1987. El Malm i el Cretaci inferior entre el Massís de Garraf i la Serra d’Espadà.  
544 Anàlisi de Conca. (Unpubl. PhD thesis). Universitat de Barcelona, 345 pp.
- 545 Salas, R., Guimerà, J., Mas, R., Martín-Closas, C., Meléndez, A., Alonso, A., 2001.  
546 Evolution of the Mesozoic Central Iberian Rift System and its Cainozoic inversion  
547 (Iberian Chain). In: Ziegler, P.A., Cavazza, W., Roberston, A.H.F., Crasquin-  
548 Soleau, S. (Eds.), Peri-Tethys Memoir 6: Peri-Tethyan Rift/Wrench Basins and

549 Passive Margins. Mémoires du Muséum National d'Histoire Naturelle, Paris 186,  
550 145–186.

551 Salas, R., García-Senz, J., Guimerà, J., Bover-Arnal, T., 2010. Opening of the Atlantic and  
552 development of the Iberian intraplate rift basins during the late Jurassic-early  
553 Cretaceous. II Central and North Atlantic Conjugate Margins Conference, 245–248.

554 Salas, R., Casas, A., 1993. Mesozoic extensional tectonics, stratigraphy, and crustal  
555 evolution during the Alpine cycle of the eastern Iberian basin. *Tectonophysics*, 228,  
556 33–55.

557 Salas, R., Guimerà, J., 1996. Rasgos estructurales principales de la cuenca Cretácica  
558 Inferior del Maestrazgo (Cordillera Ibérica oriental). *Geogaceta*, 20, 1704–1706.

559 Straelen, V. van, 1925. Contribution à l'étude des crustacés décapodes de la période  
560 Jurassique. *De Académie Royale de Belgique, Classe des Sciences, Mémoires*, 2(7),  
561 1–462.

562 Straelen, V. van, 1927. Contribution à l'étude des crustacés décapodes de la Péninsule  
563 ibérique. *Eos*, 3, 69–79.

564 Straelen, V. van, 1936. Crustacés décapodes nouveaux ou peu connus de l'époque  
565 crétacique. *Bulletin du Muséum royale d'Histoire naturelle de Belgique*, 12(45), 1–  
566 50.

567 Schweitzer, C.E., Feldmann, R.M., Garassino, A., Karasawa, H., Schweigert, G., 2010.  
568 Systematic List of Fossil Decapod Crustacean Species. *Crustacea Monographs*, 10,  
569 1–230.

570 Steuber, T., 1999. Isotopic and chemical intra-shell variations in low-Mg calcite of rudist  
571 bivalves (Mollusca: Hippuritacea): disequilibrium fractionations and Late  
572 Cretaceous seasonality. *International Journal Earth Sciences*, 88, 551–570.

- 573 Steuber, T., 2001. Strontium isotope stratigraphy of Turonian-Campanian Gosau-type  
574 rudist formations in the Northern Calcareous and Central Alps (Austria and  
575 Germany). *Cretaceous Research*, 22, 429–441.
- 576 Steuber, T., Korbar, T., Jelaska, V., Gusic, I., 2005. Strontium isotope stratigraphy of  
577 Upper Cretaceous platform carbonates of the island of Brač (Adriatic Sea, Croatia):  
578 implications for global correlation of platform evolution and biostratigraphy.  
579 *Cretaceous Research*, 26, 741–756.
- 580 Vega, F.J., Feldmann, R.M., Etayo-Serna, F., Bermúdez-Aguirre, H.D., Gómez, J., 2008.  
581 Occurrence of *Meyeria magna* McCoy, 1849 in Colombia: a widely distributed  
582 species during Aptian times. *Boletín de la Sociedad Geológica Mexicana*, 60, 1–10.
- 583 Woods, H., 1925-31. A monograph of the fossil macrurous Crustacea of England. parts 11-  
584 VII. *Palaeontogr. Soc. Monogr.* (1925), 17–40; (1926), 4–48; (1927), 49–64;  
585 (1928), 65–72; (1930), 73–88; (1931), 89–122.
- 586 Woodward, H., 1900. Further notes on podophthalmous crustaceans from the Upper  
587 Cretaceous formation of British Columbia. *Geological Magazine, New Series*, 7,  
588 432–435.
- 589 Zittel, K.A. von, 1885. *Handbuch der Palaeontologie*, 1(2). Mollusca und Arthropoda.  
590 München and Leipzig: R. Oldenbourg, 893 pp.

591

592

593

### FIGURE CAPTIONS

594

595 Fig. 1. (A) Geographical situation of the Maestrat Basin in the eastern Iberian Chain (E Iberian Peninsula).

596 (B) Simplified palaeogeographic and structural map of the Maestrat Basin during the Late Jurassic-Early

597 Cretaceous rifting cycle and location of the study area in La Salzedella sub-basin. Mo: Morella sub-basin, Pe:  
598 El Perelló sub-basin, Sa: La Salzedella sub-basin, Ga: Galve sub-basin, Ol: Oliete sub-basin, Al: Aliaga sub-  
599 basin, Pg: Penyagolosa sub-basin. Modified after Salas et al. (2001) and Bover-Arnal et al. (2014). (C)  
600 Geological map and location of the outcrop logged and sampled for *A. rapax*. Modified after Esnaola and  
601 Canérot (1972) and Canérot and Pignatelli García (1977).

602

603 Fig. 2. Stratigraphic section of the Lower Barremian sedimentary record containing specimens of  
604 *Atherfieldastacus rapax* logged in the surroundings of Ares del Maestrat in the Maestrat Basin (E Iberia). The  
605 situation of the two horizons with *A. rapax* recognized, as well as the 26 samples used for microfacies and  
606 micropalaeontological analyses and the oysters collected for strontium-isotope stratigraphy, are indicated. See  
607 Fig. 1C for location of the sedimentary log.

608 Fig. 3. Outcrop, components and textures. (A) Outcrop view of the upper part of the sedimentary succession  
609 studied in a road cut on CV-15 that goes from the town of Ares del Maestrat to Vilafranca. (B)  
610 Photomicrograph of a poorly sorted peloidal-skeletal grainstone located at the base of the succession studied.  
611 Note the presence of an ooid (red arrow). Sample V1. (C) Specimen of *Choffatella decipiens* (red arrow)  
612 occurring in a poorly sorted grainstone texture found in the lower part of the sedimentary succession  
613 analyzed. Sample V2. (D) Detail of a Dasycladacean section found in a skeletal-peloidal grainstone of the  
614 lower part of the succession investigated. Sample V2. (E) Detail of a centimeter-thick framestone texture  
615 made up of oysters and serpulids (white tubes). Meter 2.65. (F) Photomicrograph of serpulids giving rise to a  
616 framestone texture located at meter 2.65. Sample V4. (G) Detail of an oyster exhibiting *Gastrochaenolites*  
617 with the shell of the lithophagid bivalve preserved within the boring. Sample V5.

618

619 Fig. 4. Components and textures. (A) Floatstone with fragments of rocks (red arrows), mollusks and  
620 echinoids. Sample V11. (B) Detail of *Thalassinoides* occurring at the base of a limestone bed in the upper part  
621 of the succession investigated. Meter 15.45. (C) Close-up view of a scleractinian fragment within a floatstone  
622 texture dominated by shells of mollusks. Sample V19. (D) Razor clam found in the upper part of the section  
623 studied. Sample V21. (E) Photomicrograph of a skeletal wackestone to packstone texture from the tabular  
624 limestone bed marking the top of the succession examined. Red arrows point to gastropod shells. Sample

625 V26. (F) Close-up view of a crinoid fragment occurring within a skeletal wackestone to packstone texture  
626 around meter 20. Sample V26.

627

628 Table 1. Strontium-isotope stratigraphy of the oyster shells analyzed and their elemental composition. In bold  
629 the mean value of the Sr-isotope ratio of the sample set. Preferred numerical ages have been derived from the  
630 look-up table of McArthur et al. (2001, version4: 08/03), which is calibrated to the Geological Time Scale of  
631 Gradstein et al. (2004). The Early Barremian time interval comprised between the underlined preferred age of  
632 130.43 Ma and its associated minimum age of 128.54 Ma corresponds to the assigned favoured age for the *A.*  
633 *rapax* specimens (see text for further details).

634

635 Fig. 5. Morphological features and regions of the carapace in *Atherfieldastacus rapax* based on specimen  
636 MGB 76814. Anatomical abbreviations: a = branchiocardiac groove, ac = antennal carina, b = antennal  
637 groove, b<sub>1</sub> = hepatic groove = c = post-cervical groove, cd = cardiac groove, e<sub>1</sub>e = cervical groove, gc =  
638 gastro-orbital carina, hr = hepatic ridge, i = inferior groove, oc = orbital carina. Colors: blue = branchial  
639 region, green = hepatic region, yellow = pterygostomial region, orange = antennal region, red = gastric region,  
640 purple = cardiac region.

641

642 Fig. 6. *Atherfieldastacus rapax*, lateral view of specimen (MGB 76814) from Ares del Maestrat. (A) Close up  
643 of the lateral view showing the granules in the cephalothorax (for the anatomical features and regions see  
644 Figure 5). (B) Close up of the dorsal view that shows the lateral compression of the cephalothorax. (C) Close  
645 up of lateral view, it is possible to observe the orbital, gastro-orbital and antenal carinae. (D) Full view of  
646 specimen with a preserved cephalothorax and some incomplete pereopods and a small part of the abdomen.

647

648 Figure 7. *Atherfieldastacus rapax* MGB 76815. (A) Coated with ammonium chloride. (B) Non-coated. The  
649 figure shows the morphological features in the cephalothorax; the pleon is separated from the cephalothorax.  
650 Some slender pereopods can be observed disjointed from the body.

651

652 Figure 8. Schemes that show the differences between the arrangement of the three rostral carinae in (A)  
653 *Atherfieldastacus rapax* and (B) *Atherfieldastacus magnus*. B modified from González-León et al., 2016.

654

655 Figure 9. *Atherfieldastacus rapax*. Specimen MGB 78616 (A) Full view of specimen showing part of the  
656 branchial region of cephalothorax, five triangular abdominal pleuras incomplete and telson. (B) Close up of  
657 the telson showing uropodal endopodite and serrated exopodite with dieresis. (C) Close up of the abdomen  
658 showing the granulation and serrated edges of the abdominal pleuras.

659

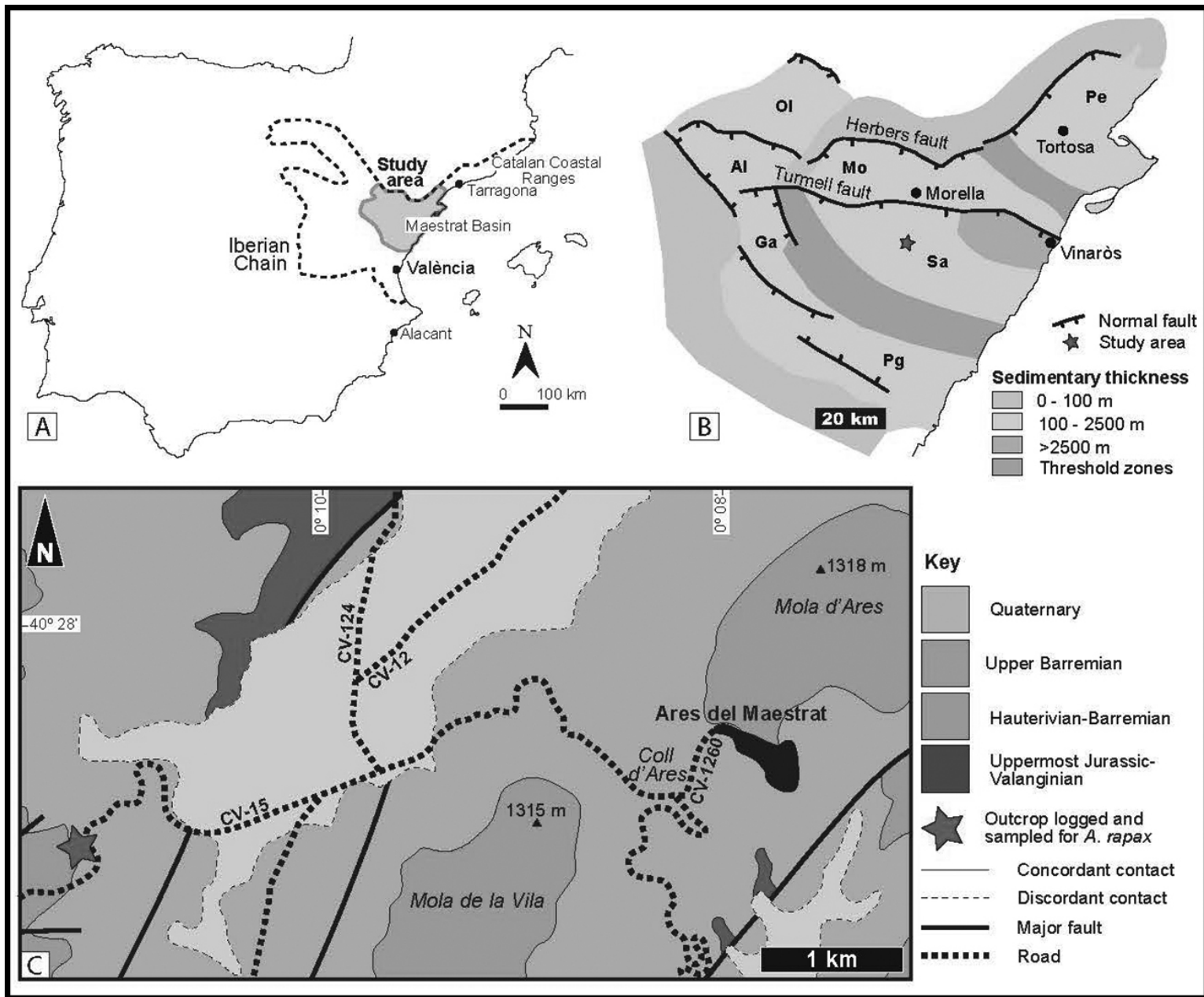
660 Appendix 1. *Meyeria rapax* early Valanginian of Sachsenhagen locality, Germany; specimens located in a  
661 private collection ([www.starkefossilien.de](http://www.starkefossilien.de)). A-C) Show some features presents in the Spanish specimens:  
662 oc=orbital carinae, gc=gastro-orbital carinae, ac=antennal carinae, hr=hepatic ridge, r2=dorsal branchial ridge  
663 and r3=medial branchial ridge. Dimensions: A) 15 cm, B) 16 cm and C) 22 cm.

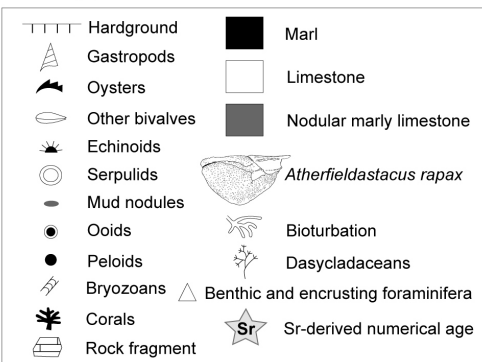
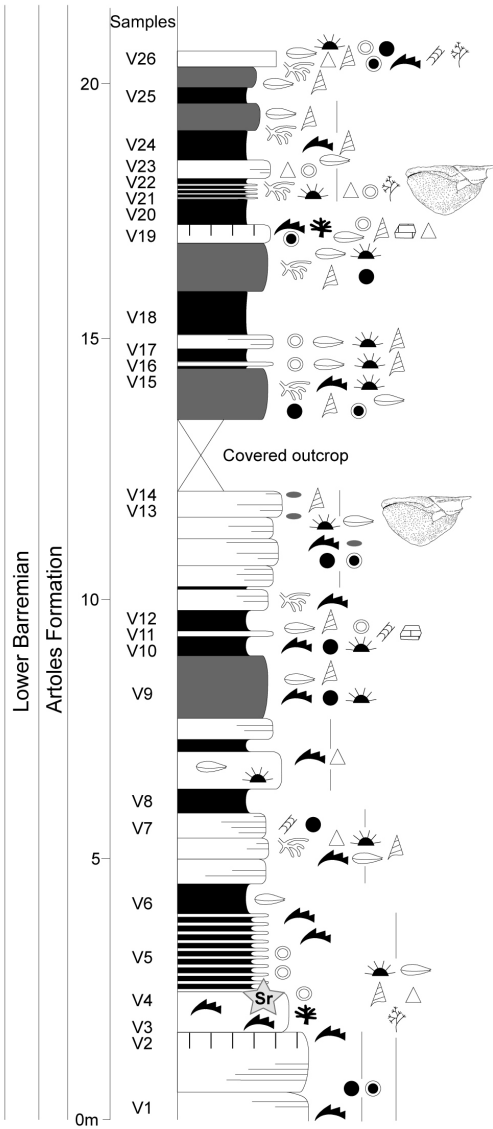
664

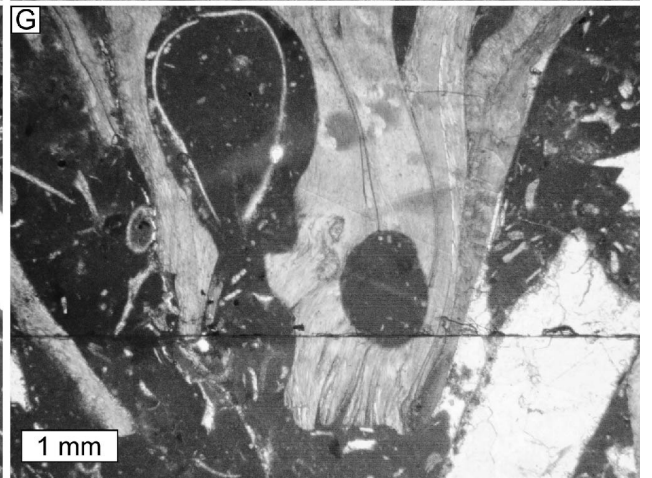
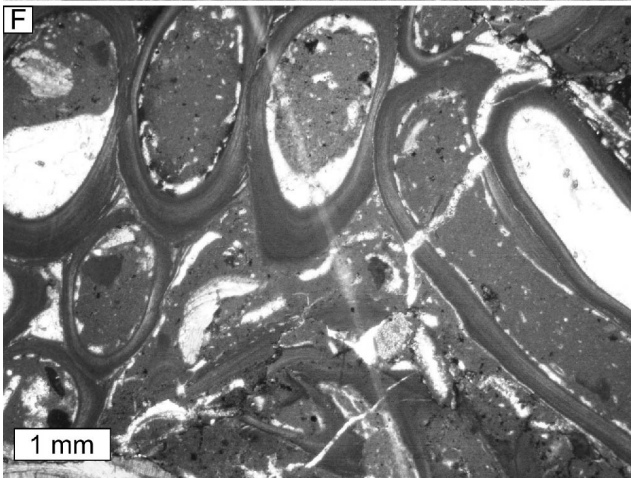
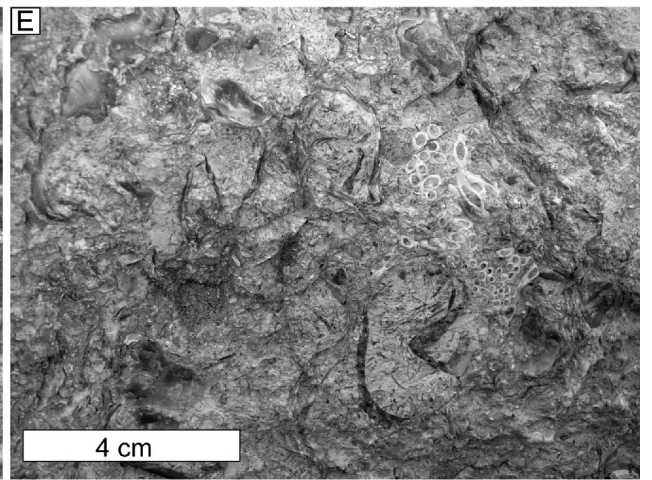
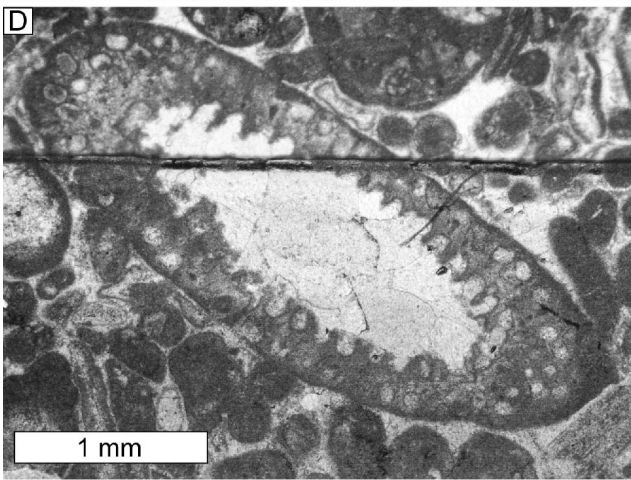
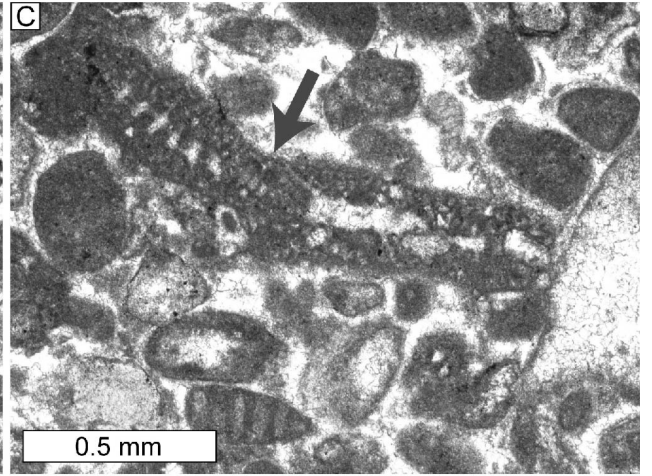
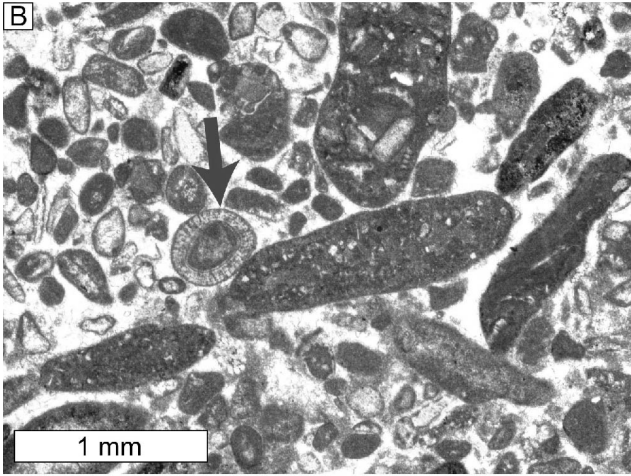
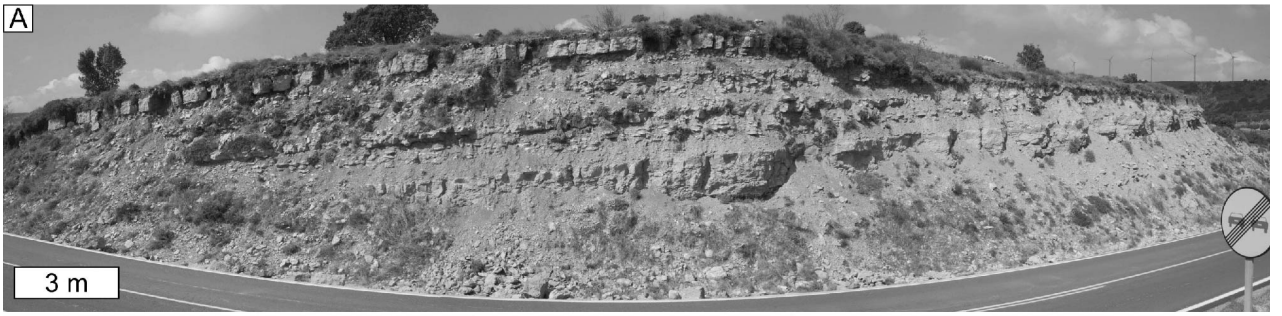
665

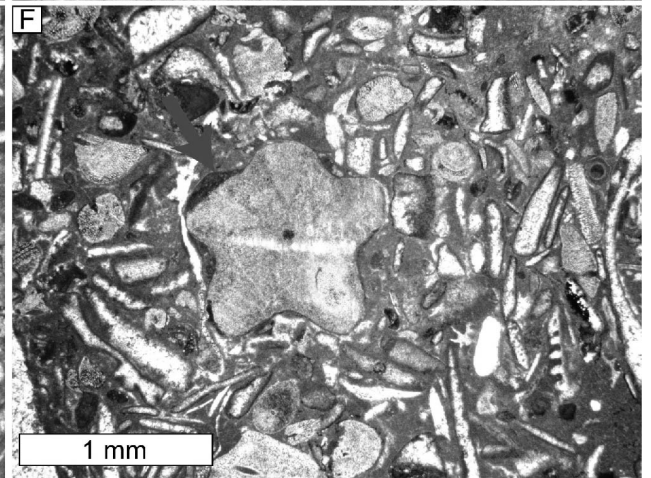
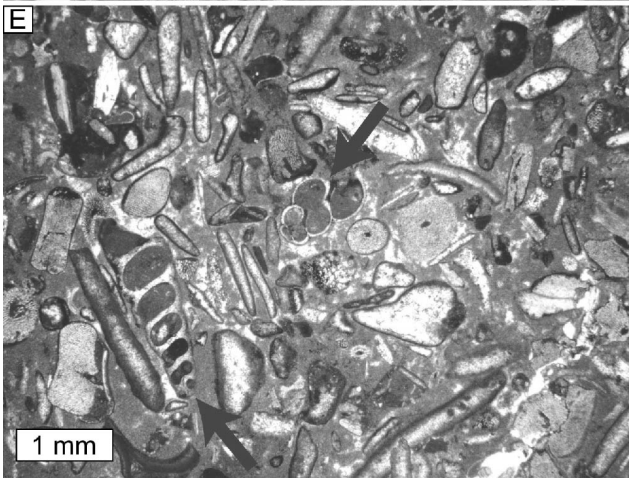
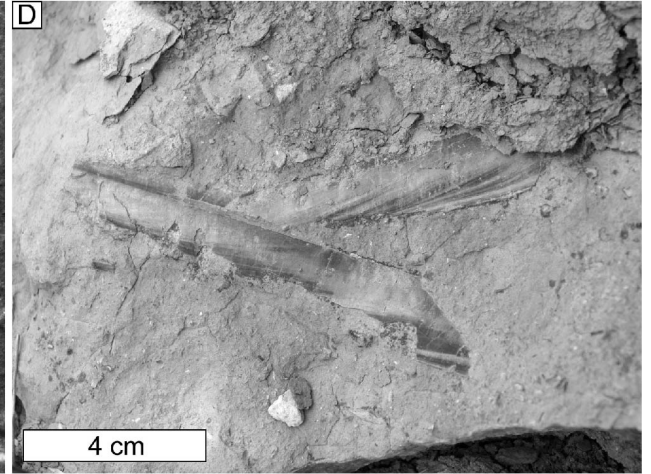
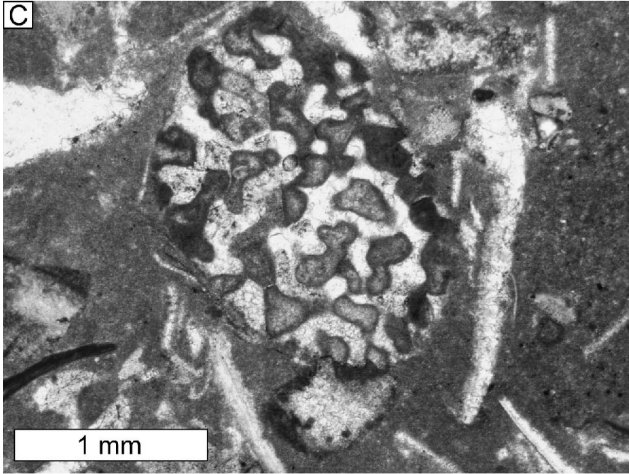
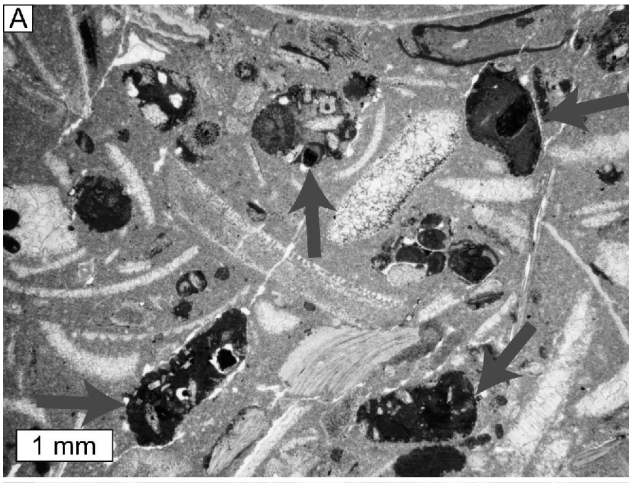
666

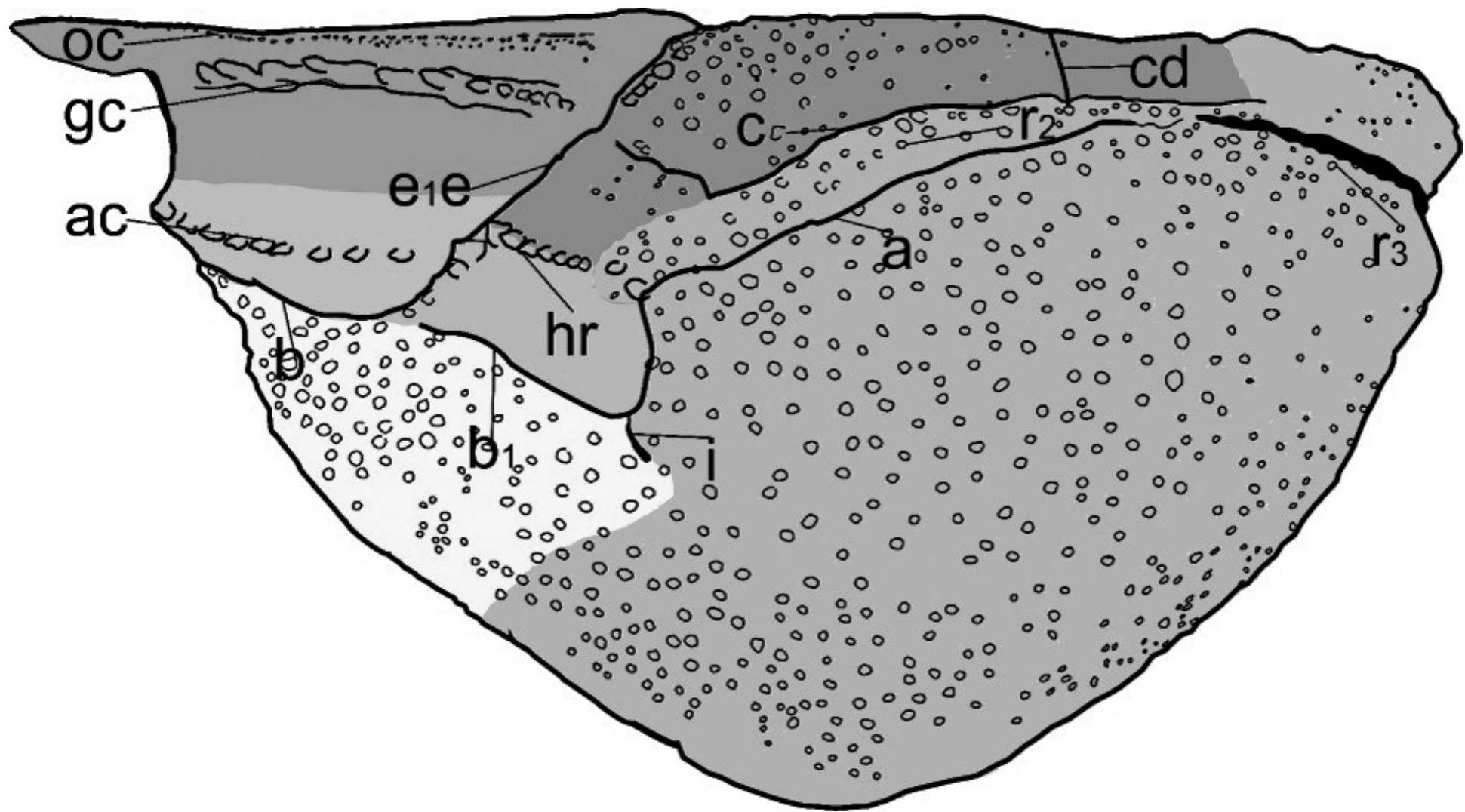
667

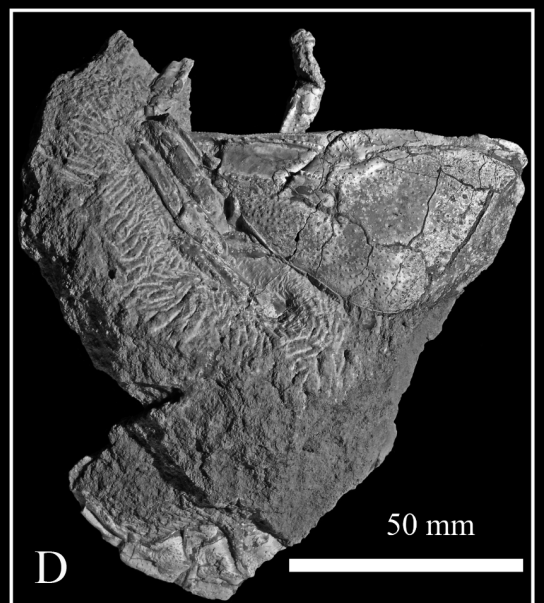
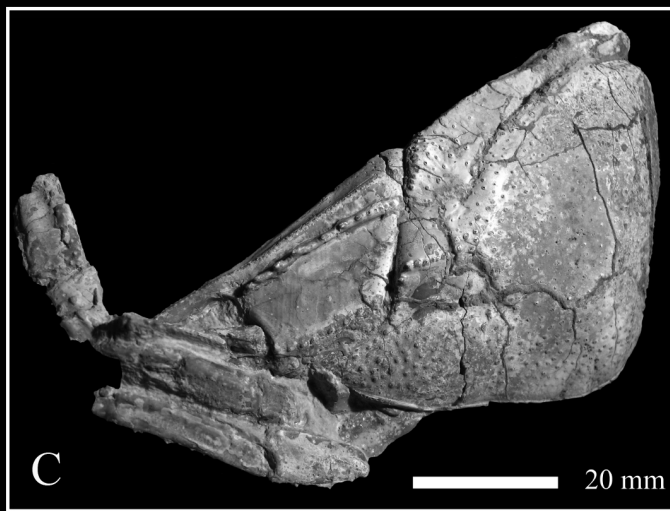
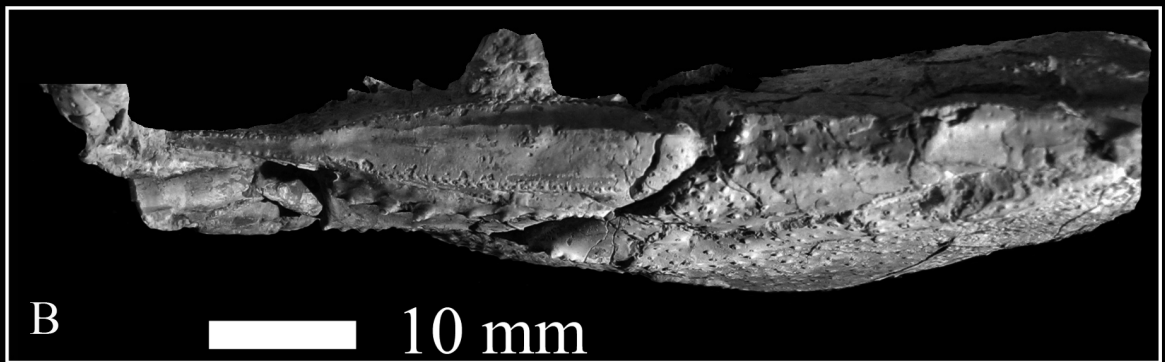
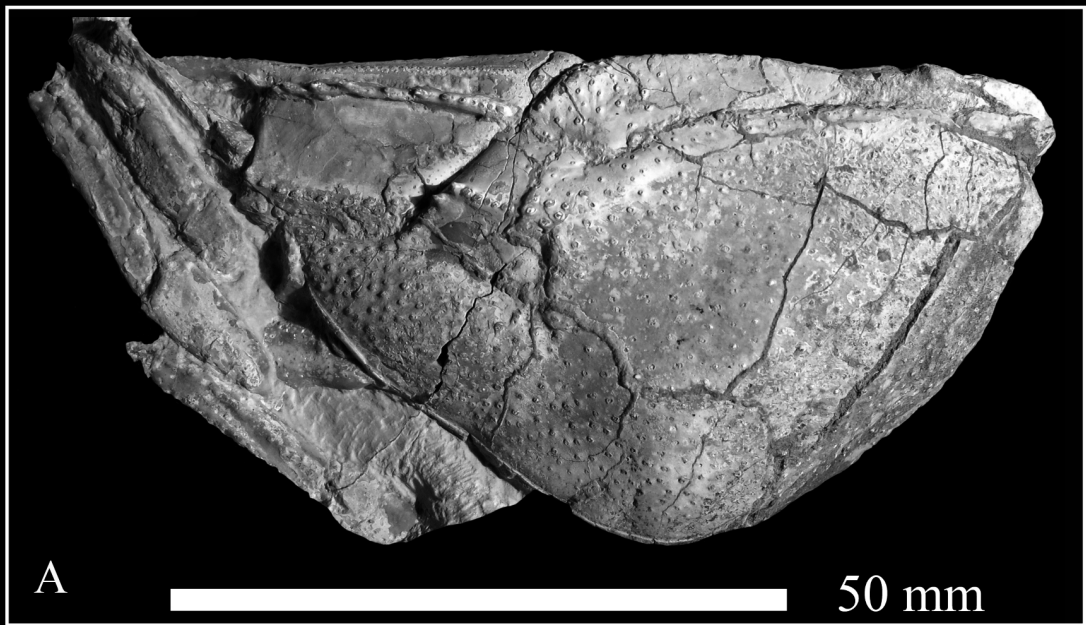






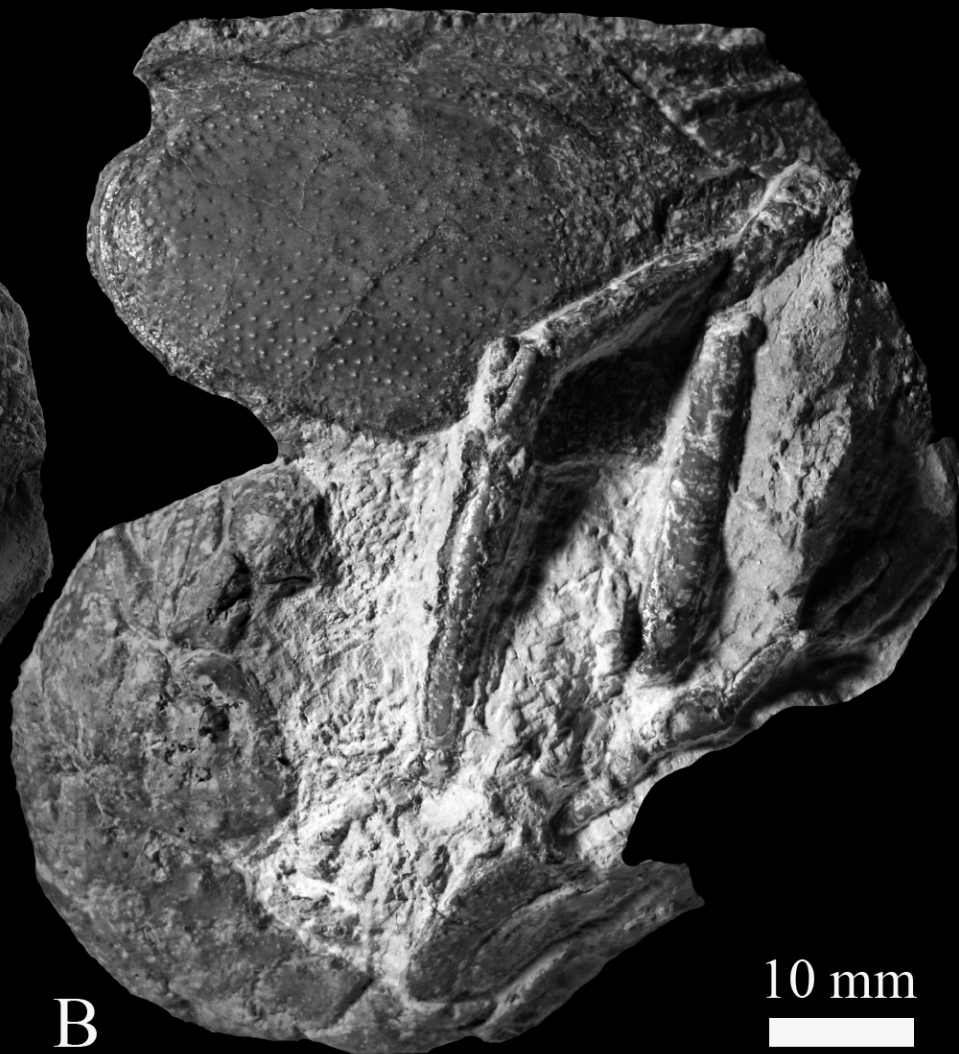








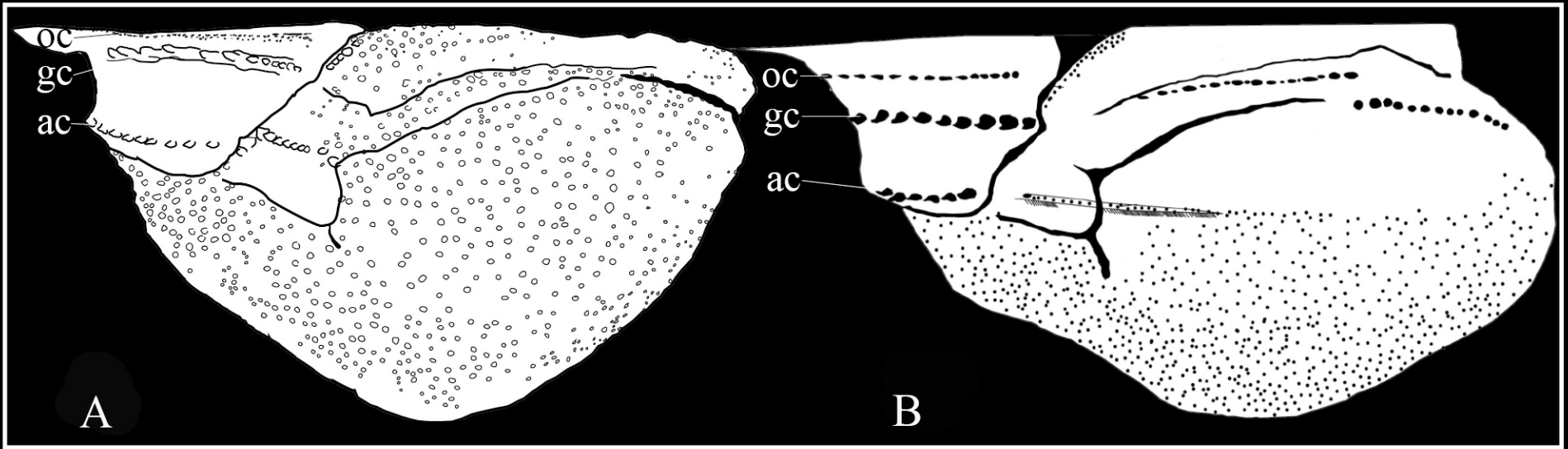
A

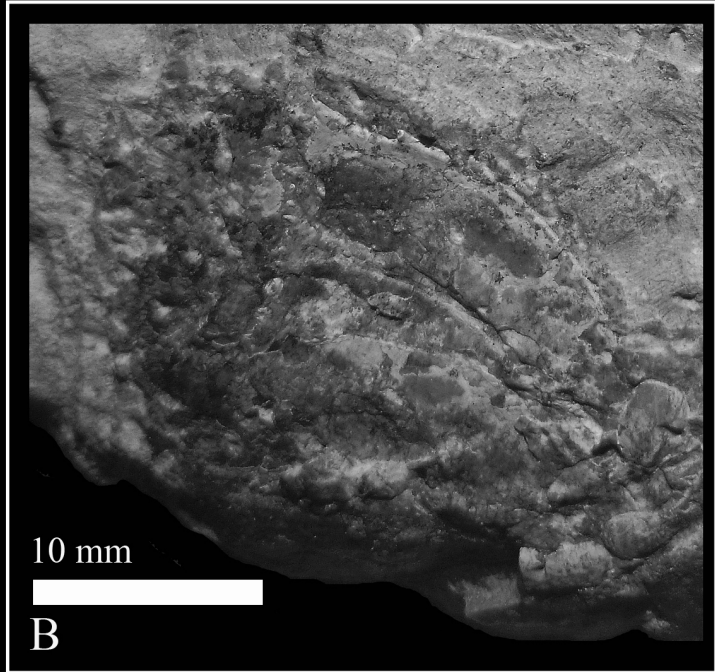
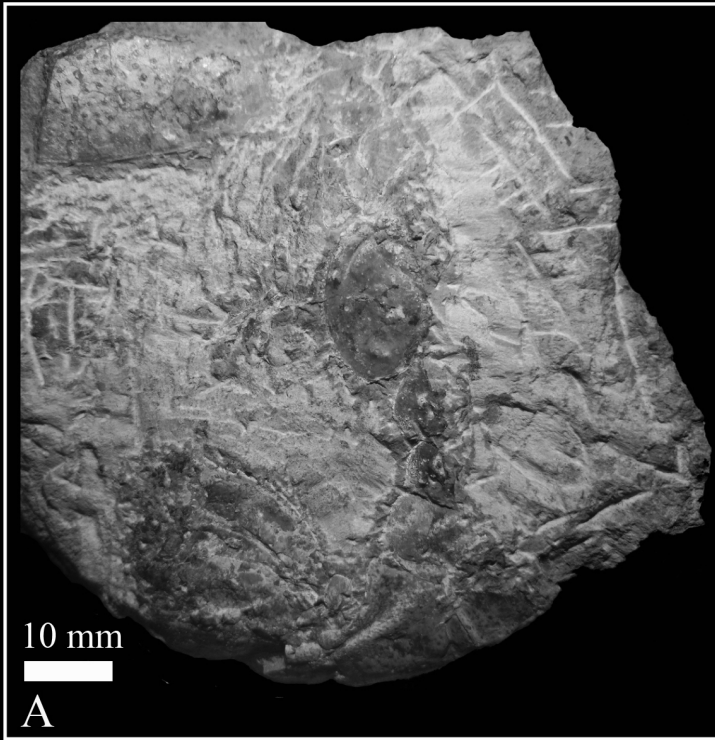


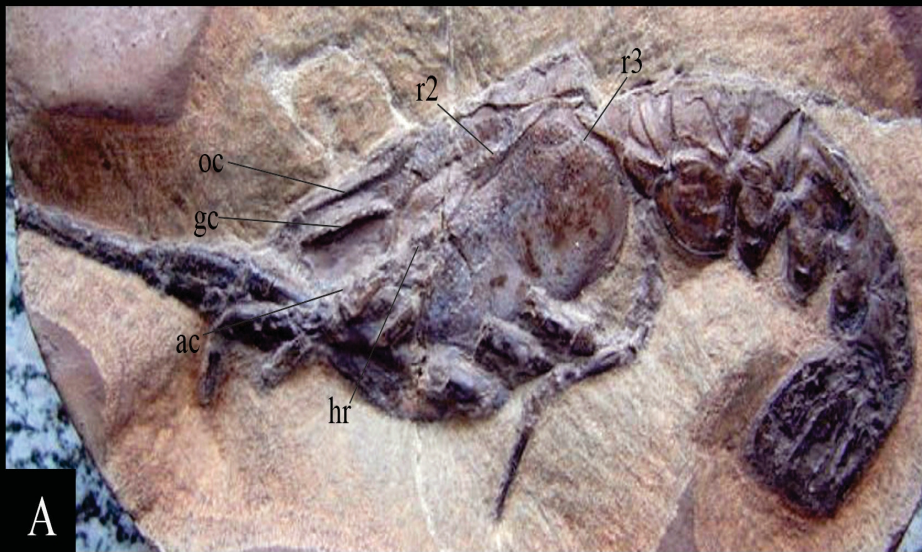
B

10 mm

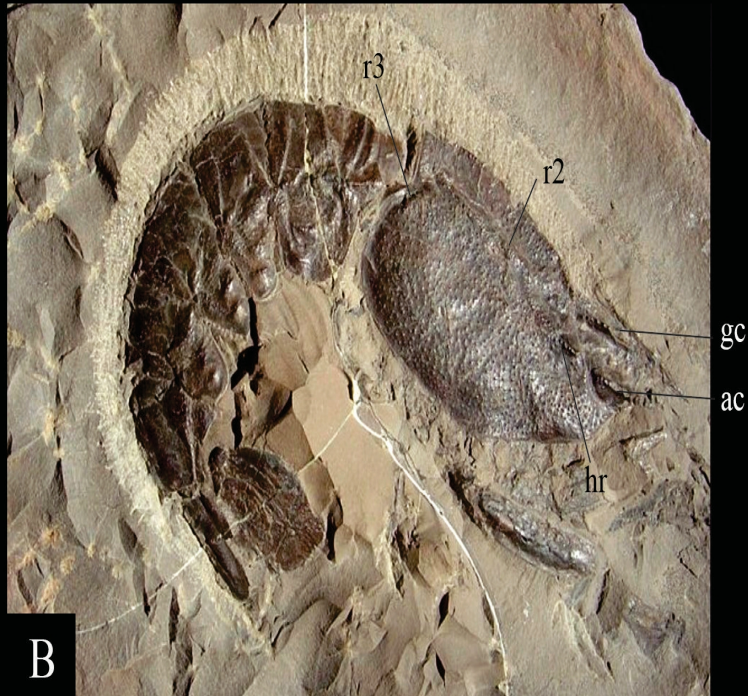








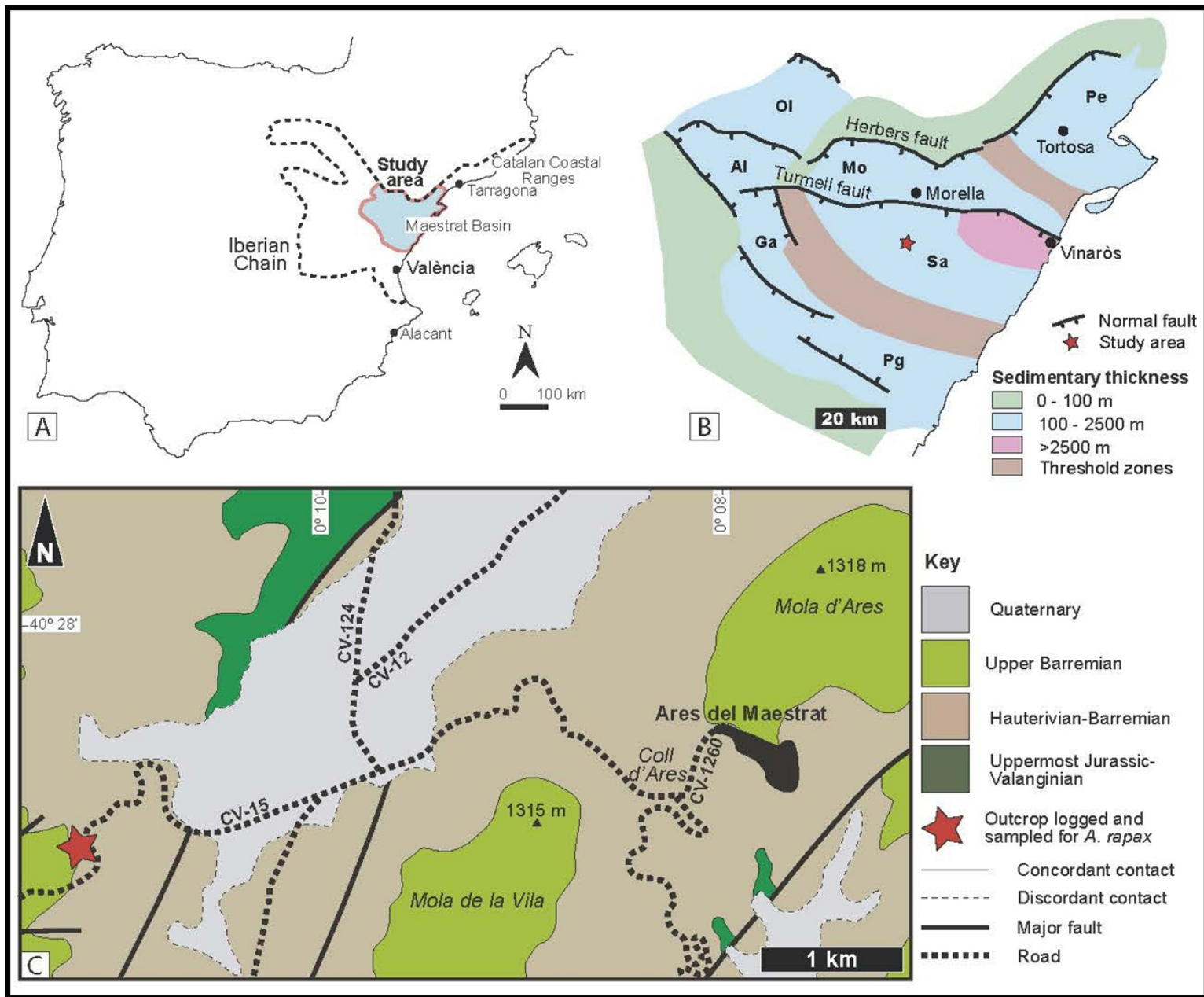
A

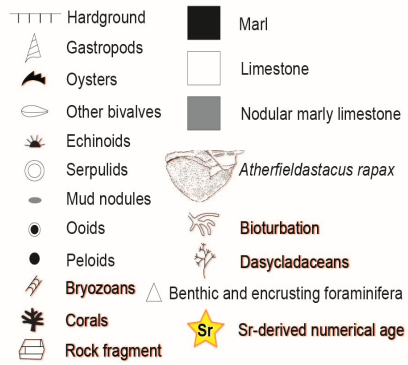
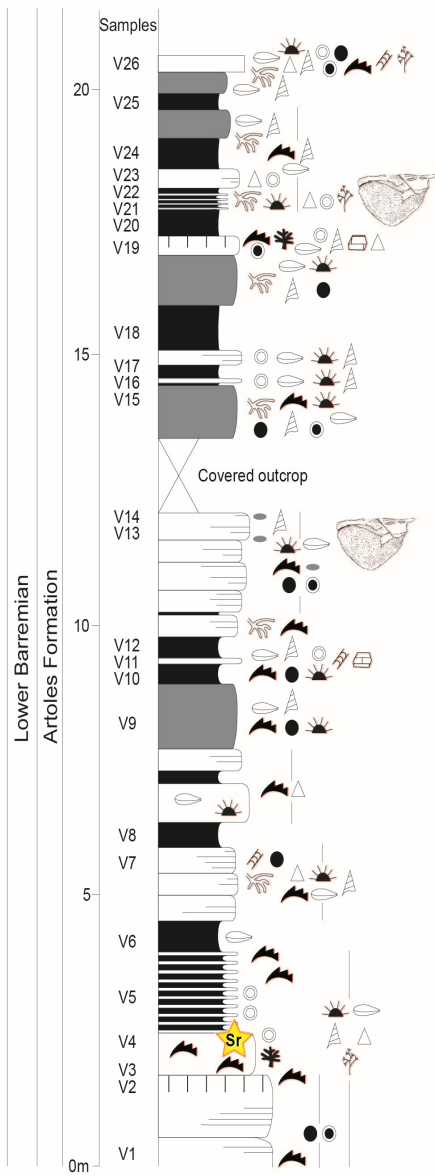


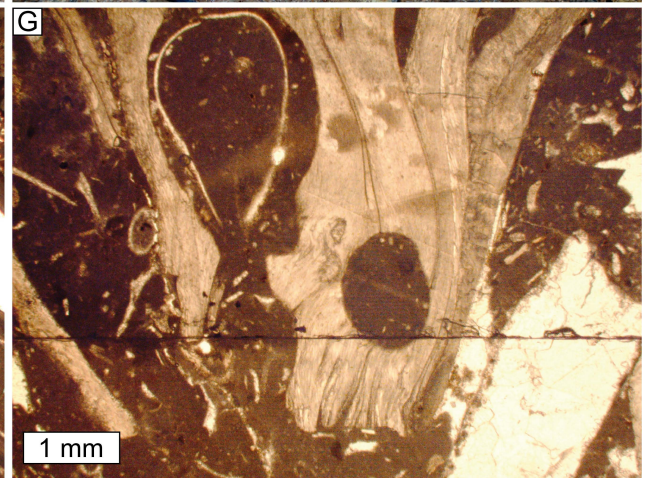
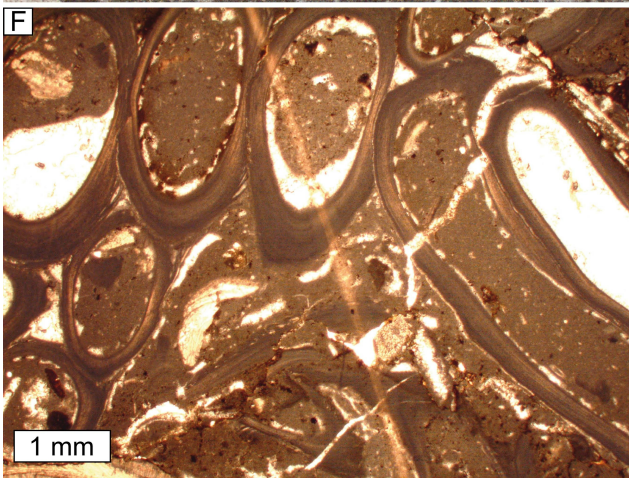
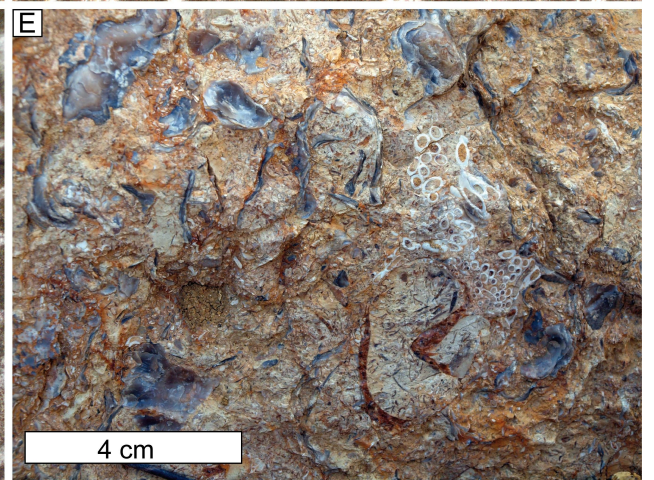
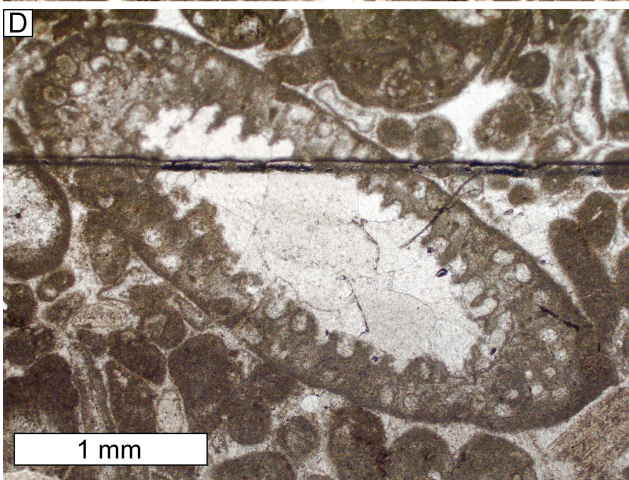
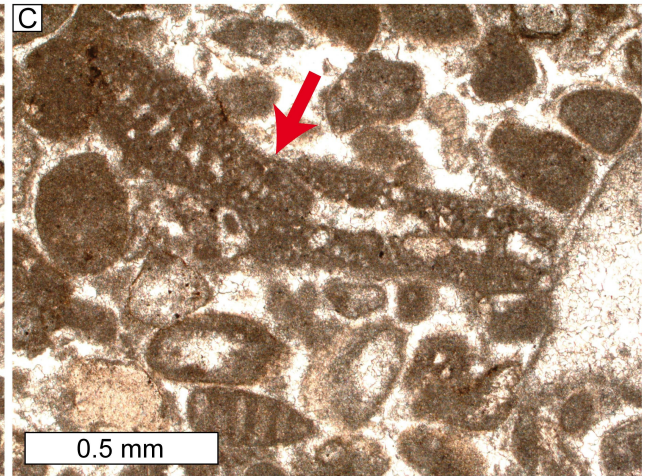
B

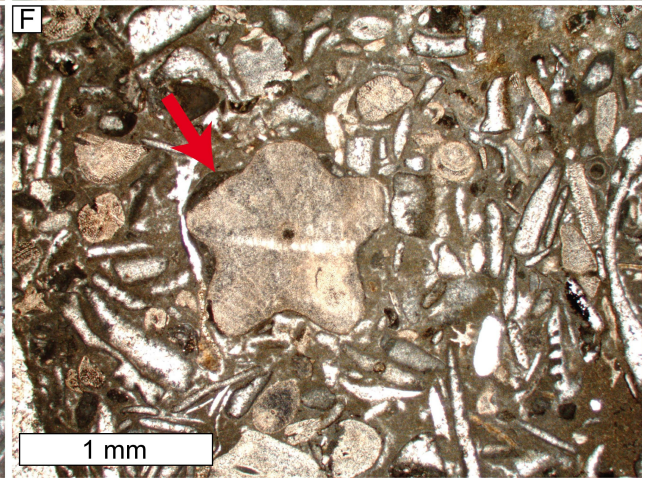
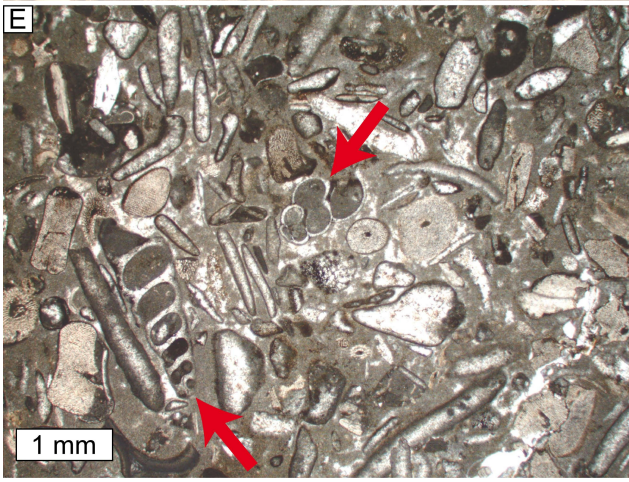
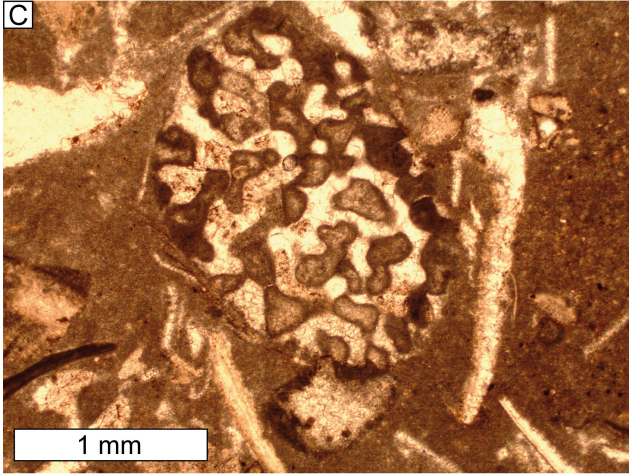
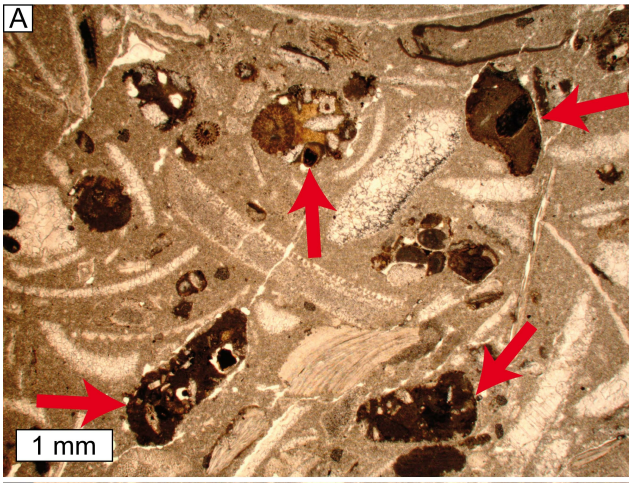


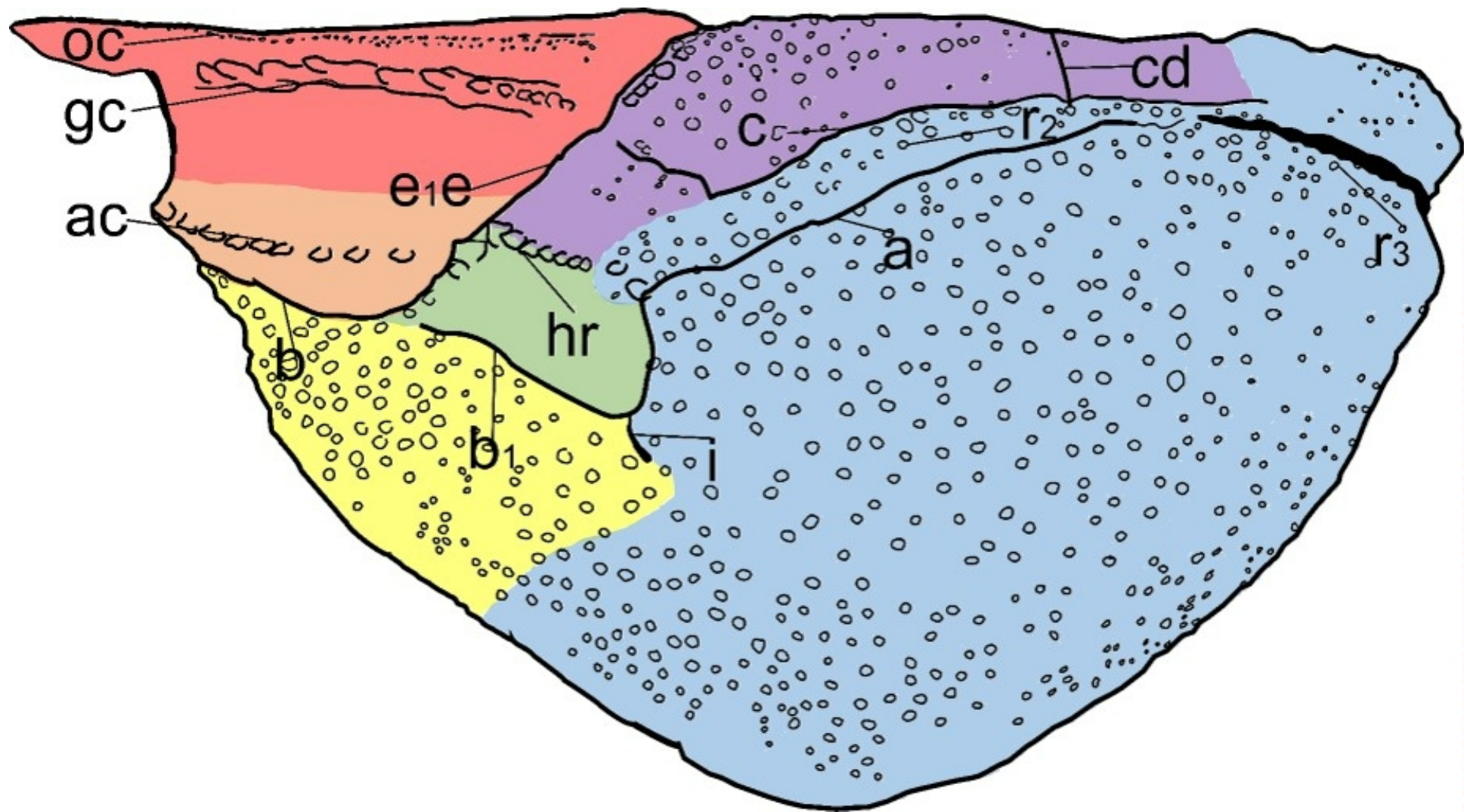
C

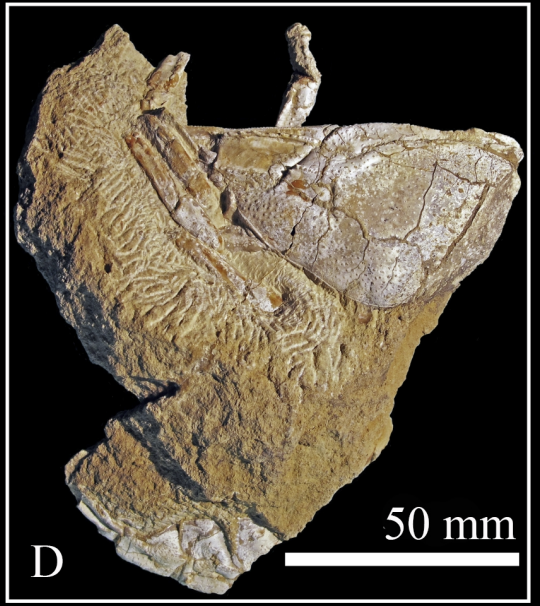
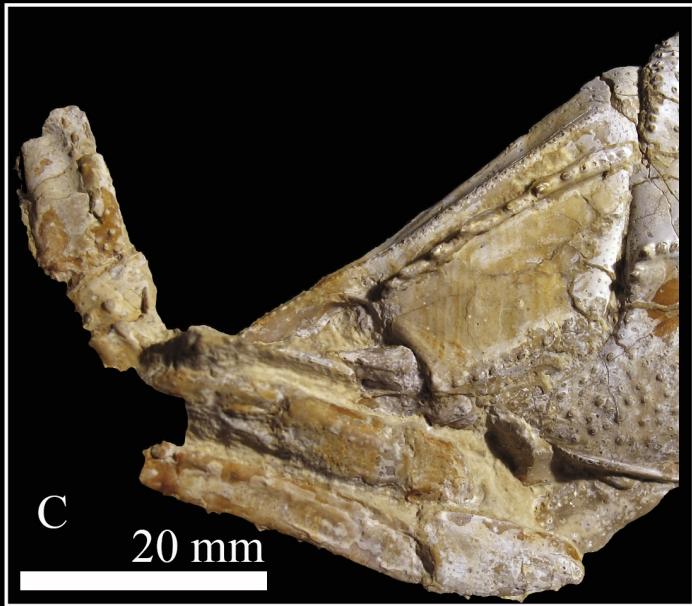
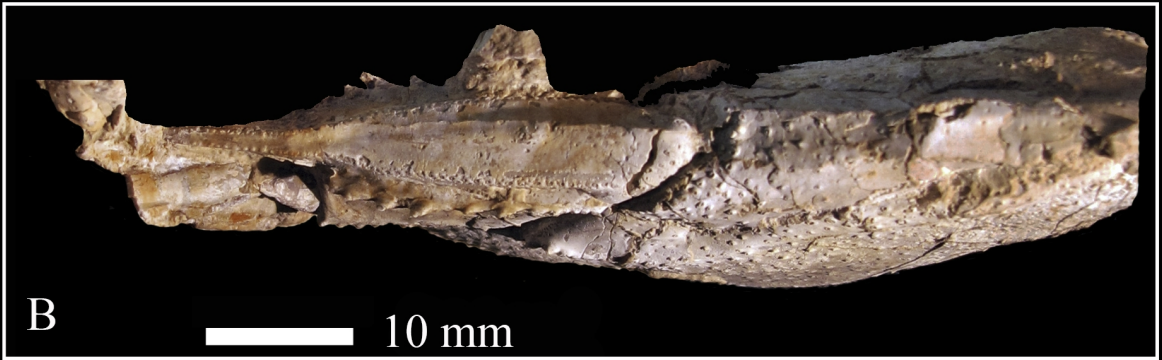
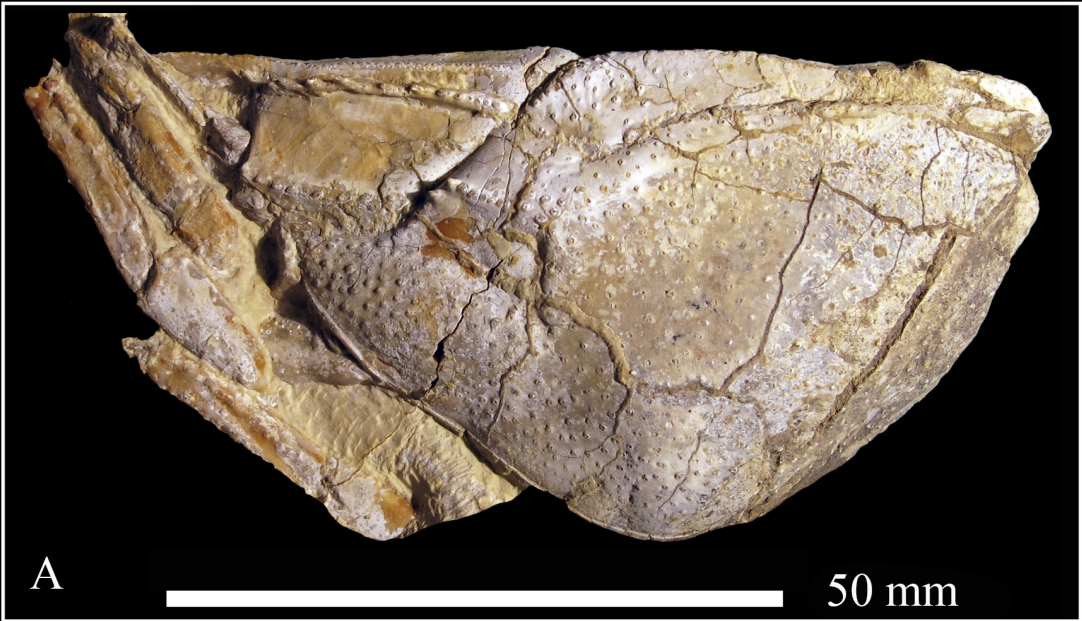














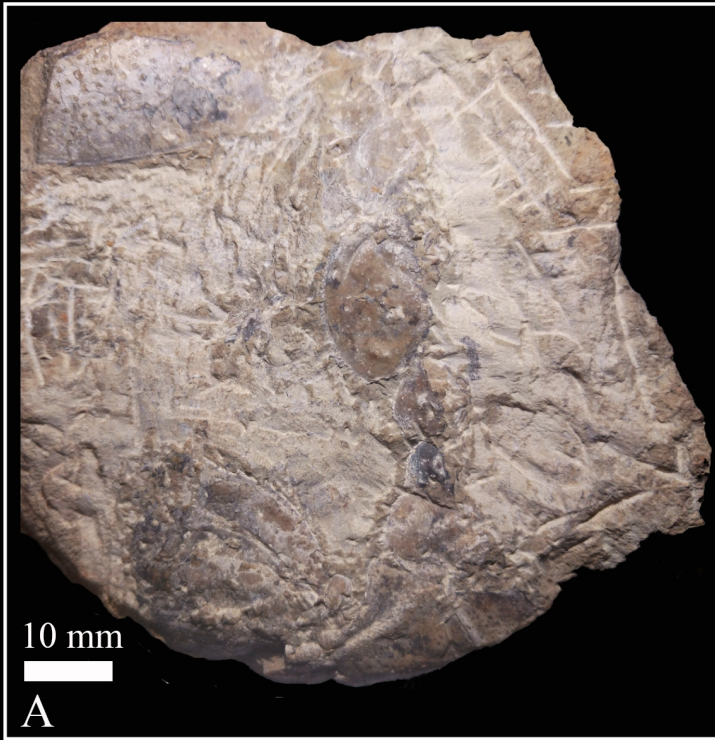
A



B

10 mm





Sample	Component	<sup>87</sup> Sr/ <sup>86</sup> Sr measured	± 2 se sample	<sup>87</sup> Sr/ <sup>86</sup> Sr corrected	± 2 se mean sample values	Ca ppm	Mg ppm	Sr ppm	Fe ppm	Mn ppm	min	Age (Ma)	max	Stage
V4A	Oyster	0,707454	0,000005	0,707468		391480	673	797,5	96,4	21,8				
V4B	Oyster	0,707461	0,000005	0,707475		392500	1050	846,9	83,0	26,3				
			mean	<b>0,707472</b>	0,000011						128,54	<u>130,43</u>	131,83	latest Hauterivian / Early Barremian
											125,86	126,46	127,27	Late Barremian

Sample	Component	<sup>87</sup> Sr/ <sup>86</sup> Sr measured	± 2 se sample	<sup>87</sup> Sr/ <sup>86</sup> Sr corrected	± 2 se mean sample values	Ca ppm	Mg ppm	Sr ppm	Fe ppm	Mn ppm	min	Age (Ma)	max	Stage
V4A	Oyster	0,707454	0,000005	0,707468		391480	673	797,5	96,4	21,8				
V4B	Oyster	0,707461	0,000005	0,707475		392500	1050	846,9	83,0	26,3				
			mean	<b>0,707472</b>	0,000011						128,54	<u>130,43</u>	131,83	latest Hauterivian / Early Barremian
											125,86	126,46	127,27	Late Barremian

- ❖ The first occurrence of the decapod mecochirid *Atherfieldastacus rapax* (*Meyeria rapax*) of the Artoles Formation NE Spain.
  
- ❖ Microfacies and paleontological analyses of the sedimentary succession containing the fossil lobsters allow us to infer a near-coastal depositional setting.
  
- ❖ Numerical ages derived from Sr-isotope analyses combined with previous chronostratigraphic studies of the Artoles Formation suggest an Early Barremian age for the stratigraphic interval.
  
- ❖ Morphological features in the Spanish specimens allows us included this material in the new genus recently proposed “*Atherfieldastacus*”.